C. elegans ADAMTS ADT-2 regulates body size and cuticle collagen organization

by

Thilini Fernando

A dissertation submitted to the Graduate Faculty in Biology in partial fulfillment of the requirements for the degree of Doctor of Philosophy, The City University of New York

2010

This manuscript has been read and accepted for the
Graduate Faculty in Biology in satisfaction of the
dissertation requirement for the degree of Doctor of Philosophy.

Dr. Cathy Savage-Dunn
Chair of Examining Committee

Dr. Laurel A. Eckhardt
Executive Officer

Dr. Alicia Melendez
Dr. Daniel Weinstein
Dr. Monica Driscoll
Dr. Hannes Buelow
Supervisory Committee

THE CITY UNIVERSITY OF NEW YORK

Abstract

C. elegans ADAMTS ADT-2 REGULATES BODY SIZE AND CUTICLE COLLAGEN ORGANIZATION

by

Thilini Fernando

Advisor: Professor Cathy Savage-Dunn

The regulation of body size is a fundamental feature of animals critical to their survival and fitness, yet its underlying mechanisms remain poorly understood. In *C. elegans*, the DBL-1 signaling pathway plays a major role in growth control. The mechanisms by which other pathways regulate body size function, however, are less well understood. To identify additional genes involved in body size regulation, a genetic screen for small mutants was previously performed. One of the genes identified in that screen was *sma-21*. I now demonstrate that *sma-21* encodes ADT-2, a member of the ADAMTS (a disintegrin and metalloprotease with thrombospondin motifs) family of secreted metalloproteases. ADAMTS proteins are believed to remodel the extracellular matrix (ECM) and may modulate the activity of extracellular signals. Genetic interactions suggest that ADT-2 acts in parallel with known size regulatory pathways. I further demonstrate that ADT-2 activity is required for normal cuticle collagen fibril organization and *adt-2* regulatory sequences drive expression in glial-like cells. ADT-2::GFP fusion protein is localized in the alae and the annuli of the cuticle. We therefore show that ADT-2 is secreted into the cuticle where it may act to proteolytically process secreted collagen or other ECM molecules required for normal cuticle structure and body size.

Acknowledgements

I am very grateful to my mentor Dr. Cathy Savge-Dunn, because if it was not for her immense support, guidance and knowledge I could not have gotten it done.

I want to sincerely thank Dr. Alicia Melendez and Dr. Hannes Bülow for their valuable suggestions and support throughout my Ph.D. studies. I would not have cloned the gene without their help. I would also like to thank my committee members, Dr. Monica Driscoll and Dr. Daniel Weinstein for their suggestions throughout the project.

I am also thankful to my friends in the lab, particularly, Jiangha, Sheng, Edlira and Ling, who were always willing to help. I also want to thank to everyone in the Department of Biology at Queens College for their support, particularly, Dr. Tim Short and Dr. Areti Tsiola.

I want to thank my mother Chandra and my father Freddie for the enormous work load they do at home to take care of my babies so I can peacefully go to the lab and concentrate on my studies.

Finally, I want to thank the most important person behind my success, my husband Mahen. I want to thank him for three important reasons. First, for moving from LA to NY to help me finish school. Second, for the all the support and encouragement throughout the past five years. Third, for being such a kind hearted person and always trying to convince me that I did a good job.

Some of the experiments were done with equipment from the Core Facilities for Imaging, Cellular and Molecular Biology at Queens College.

Table of Contents

List of Tables

List of Figures

Introduction

I. *C. elegans* is an excellent model organism

Caenorhabditis elegans is a small free living soil nematode. It can be grown in the laboratory on petri plates with *Escherichia coli* as a food source. Sydney Brenner began using *C. elegans* for the study of development and neurobiology in the 1960's. Like other multicellular organisms, *C. elegans* undergoes developmental processes such as embryogenesis, morphogenesis and growth. Therefore, the information that we gain from *C. elegans* could be applied to higher organisms, such as humans, which are more difficult to use in laboratory experiments.

C. elegans is an excellent model system for the study of genetics and development. It has a short life cycle (3.5 days at 20^0 C) and large brood size that leads to ease of genetic analysis. The developmental pattern of all of its somatic cells has been traced. Therefore, the studying of cell signaling at the individual cell level is possible (Sulston et al., 1983; Kimble et al., 1979, Savage-Dunn, 2001). Its transparent body allows *in vivo* studies of the cells, including the behavior of individual cells and gene expression patterns.

Unlike many other animals, *C. elegans* does not have male and female sexes. Instead, there are males and hermaphrodites. A single hermaphrodite can self-fertilize and produce a large number of eggs per day. If crosses need to be carried out, hermaphrodites can be mated with males. The *C. elegans* genome size is relatively small (9.7×10^7 base pairs), when compared to the human genome which is estimated to consist of 3 billion base pairs (http://avery.rutgers.edu/WSSP/StudentScholars/project/introduction/worms.html). The entire *C. elegans* genome has been sequenced and can be used as molecular genetic toolbox. Many of

these genes have functional similarities to genes in humans and signaling pathways are also conserved. This makes *C. elegans* a powerful model system to study human disease.

II. Life cycle of the *C. elegans*

The life cycle of *C. elegans* has two parts: embryonic and postembryonic development. The length of the life cycle depends on the temperature. It has four larval stages: L1, L2, L3 and L4. At 20 ^{0} C, embryogenesis requires about 18 hours and the development from L1 to adult takes about 46 hours. At 25 ^{0} C embryogenesis requires about 14 hours and development from L1 to adult takes about 36 hours (http://www.biology.mcgill.ca/labs/roy/lifecycle.htm). In addition to these four larval stages, there is an alternative L3 larval stage named the dauer stage designed to endure unfavorable environmental conditions such as high temperature, shortage of food and high population density. Under favorable conditions dauer larvae reenter the L4 stage (Cassada and Russell 1975; Golden and Riddle 1984; Savage-Dunn, 2001).

III. Anatomy Structure

Similar to other nematodes, *C. elegans* has a cylindrical, unsegmented body. The body consists of an outer tube and inner tube which is separated by pseudocoelom. The outer body tube is composed of body wall, gonad, part of the nervous system, excretory and secretory systems. The inner body tube includes the pharynx, the remaining nervous system, intestine, rectum, and anus. Neurons are condensed around the pharynx, along the ventral midline and in the tail (Figure 1).

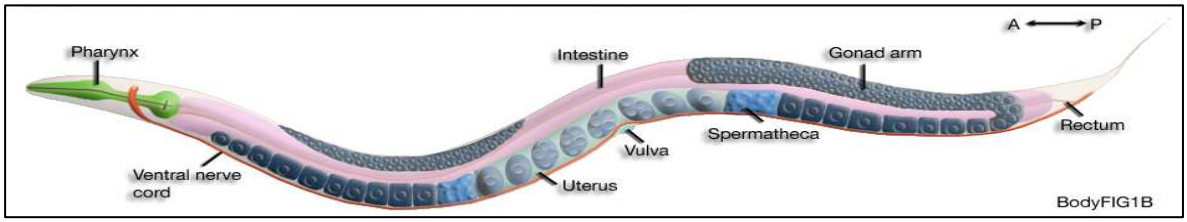

Figure 1: Schematic structure of adult hermaphrodite
(http://www.wormatlas.org/handbook/anatomyintro/anatomyintro.htm)

The hermaphrodite gonad has two arms. At the distal tip of the each arm there is a large somatic cell called distal tip cell (DTC) which guides and shapes the dividing germ cells (wormatlas). Each arm first produces sperm, which is stored in the spermatheca. Oocytes are produced next at

the distal end of the gonad. Fertilization takes place during the passage of mature oocytes through the spermatheca. Eggs are laid through the vulva at the 40 cell stage.

Adult males have a slim body and a distinctive tail that bears copulatory structures (Fig 2). Extension of the cuticle, named the fan, extends at the tail and bears 9 pairs of sensory rays. Each ray consists of two sensory neurons (A-type and B-type) and a support cell surrounded by hypodermal sheath. Each ray has individual characteristics including the morphology, position and the expression of neurotransmitters (Lints and Emmons, 1999). Rays 1, 5, and 7 are located at the dorsal side of the fan; rays 3, 6, and 9 are at the edge and rays 2, 4, and 8 at the ventral side of the fan.

Males produce only sperm and their gonad has only one arm. The anterior arm is a testis and the posterior arm includes: vas deferens; seminal vesicle; and cloaca.

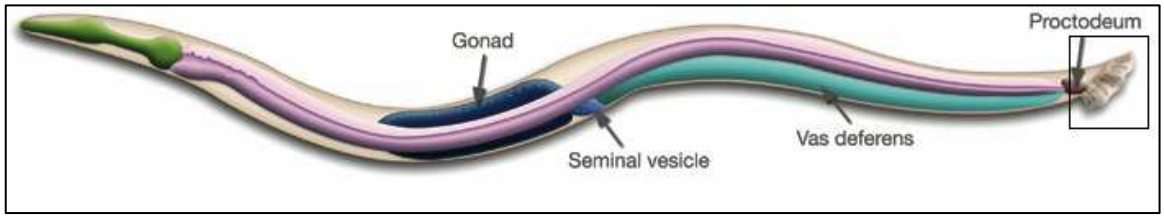

Figure 2: Schematic structure of adult male

(http://www.wormatlas.org/handbook/anatomyintro/anatomyintro.htm)

Hypodermal Cells

The body of the *C. elegans* is surrounded by hypodermal cells. Many of the hypodermal cells fuse during the development to form multinucleated syncytia. Hypodermal cells can be divided into two subtypes of cells: hypodermis (Hyp1-hpy12) and specialized epithelial cells which includes seam cells, glia - like cells and interfacial epithelial cells.

The hypodermis includes the main body syncytium, hyp7 (Figure 3). This tissue surrounds the most of the body. Smaller hypodermal cells are located in the head (hyp1 - hyp6) and the tail (hyp8 - hyp12). Two lateral rows of hypodermal cells called seam cells divide during each larval stage and one of the daughter cells fuse to the main body syncytium and the other one remains there to maintain the cell number in the seam. Hyp-7 of adult hermaphrodite contains 139 nuclei (23 embryonic nuclei, 116 postembryonic (www.wormatlas.org).

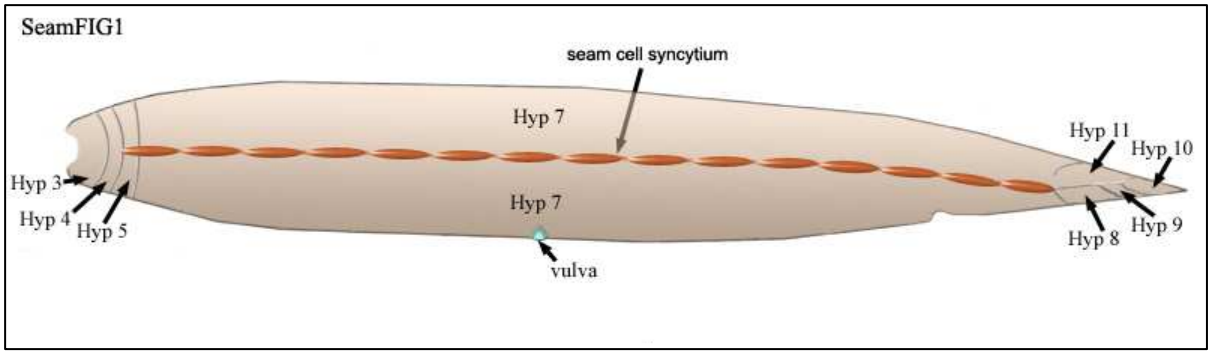

Figure 3: Hypodermis in the adult hermaphrodite (www.wormatlas.org).

Seam cells form two rows at the lateral side of the body (Figure 4). There are 10 seam cells at hatching; H0-H2, V1-V6 and T. These seam cells (except H0) have stem cell characteristics and undergo cells divisions at each larval stage. One daughter cell fuses to hyp-7 and the other one remains in the seam.

The Cuticle

The body wall consists of a cuticle secreted by the hypodermis. There are four openings which open the body to the outside through the cuticle, lips, excretory pore, vulva and the anus. The cuticle consists of a collagenous extracellular matrix (ECM). The cuticle serves several purposes for the animal: It provides protection from desiccation; It is necessary for proper body morphology and integrity; It also plays a role in locomotion by attachment to muscles (Kramer et al., 1988; Von Mende et al., 1988; Johnstone et al., 1992). Collagen in the cuticle can be grouped in to I, II, III, *dpy-7* and *dpy-2* based on the position of conserved cysteines in Gly-X-Y interruptions (Johnstone, 2000). The cuticle is synthesized five times during the development. It is first synthesized in the embryo before hatching and then at each larval stage prior to molting (Kramer, 1994). The cuticle can be subdivided into the dorsal, ventral, and lateral cuticle. The dorsal and ventral cuticle overlies the dorsal and ventral hypodermis respectively. The lateral

cuticle overlies the region containing the lateral seam cells. There are four major layers in the cuticle: epicuticle, cortical, medial and basal. The cortical region of the dorsal and the ventral cuticle consists of circumferential ridges named annuli. Lateral cuticle consists of three longitudinal ridges called alae (http://www.wormbook.org/chapters/www_cuticle/cuticle.html) (Figure 4). During the cuticle synthesis, actin filaments are formed in the hypodermal cells and organized circumferentially around the body of the worm. This organization of actin filaments is coincident with the furrows that formed in the hypodermal cell membrane and with the furrows between the annuli (Kramer, 1994). Therefore it is possible that the pattern of the actin filaments has a role in formation of annuli in the cuticle (http://www.wormbook.org/chapters/www_cuticle/cuticle.html) (Figure 5). In particular, contraction or lack of it in annuli and alae alter the body size of the animal. On one hand, annuli cause longitudinal contractions that changes the body length of the worm. On the other hand, lateral alae cause circumferential contractions that alter the width of the worm (Thein et al., 2003).

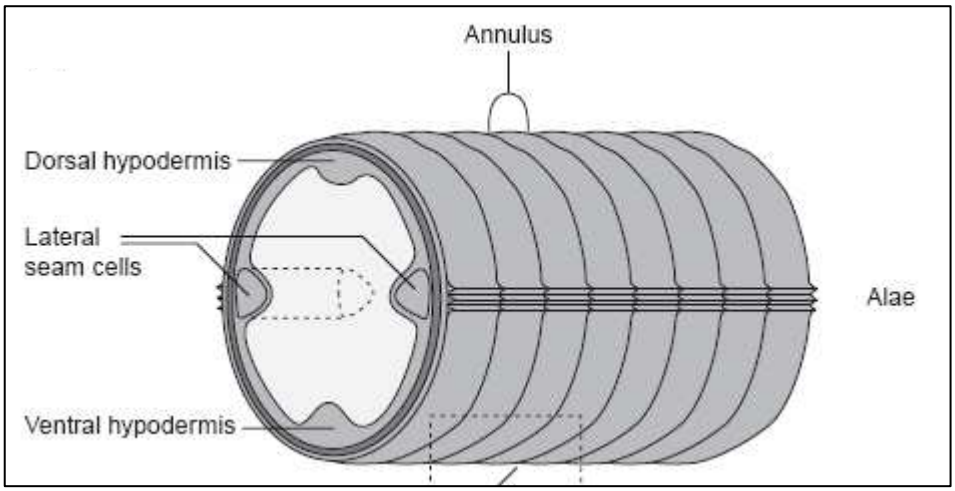

Figure 4. Structure of the cuticle (Johnstone, 2000)

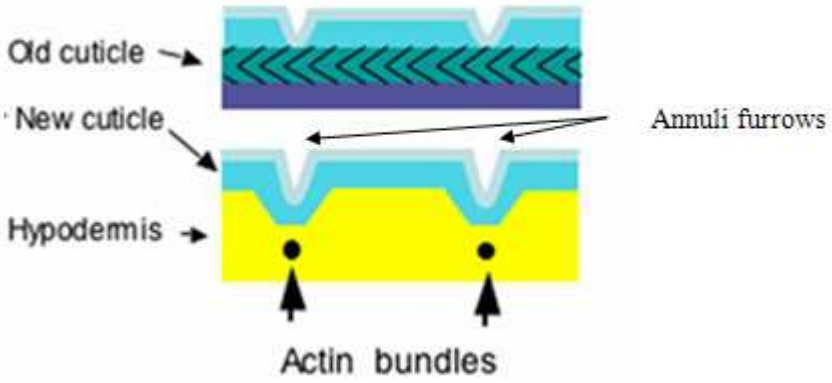

Figure 5. Annuli pattern corresponds to the pattern of actin filaments in the hypodermis (http://www.wormbook.org/chapters/www_cuticle/cuticle.html)

IV. Collagen biosynthesis pathway

Collagen biosynthesis pathway is highlighted in Figure 6. After polypeptide synthesis there will be prolyl 4-hydroxylation which allows the formation of thermally stable form of collagen. Collagen trimers will be formed via disulphide bond. This process takes place in the ER. In order to form multimers, collagen molecules have to be processed to remove N- and C- terminal propeptides. BLI-4 has been identified to be essential for the proper processing of the N-terminus propeptide (Yang and Kramer, 1994). Other than BLI-4 (subtilisin-like serine protease), collagen in *C. elegans* might also be processed by zinc metalloproteases as in vertebrates. C-terminal processing of procollagen is achieved by astacin family of zinc metalloproteases, *dpy-31*. Removal of the propeptide is necessary for the proper assembly of collagen in the ECM. It has been also found that in mammals assembly of unprocessed collagen causes the skin to be fragile. These unprocessed collagen monomers are thin and do not undergo proper crosslinking (Tang, 2001; Wang et al., 2006; Visse et al., 2003). Final step in collagen biosynthesis is crosslinking of collagen via non reducing di- and tri- tryrosine cross-links to form final insoluble matrix.

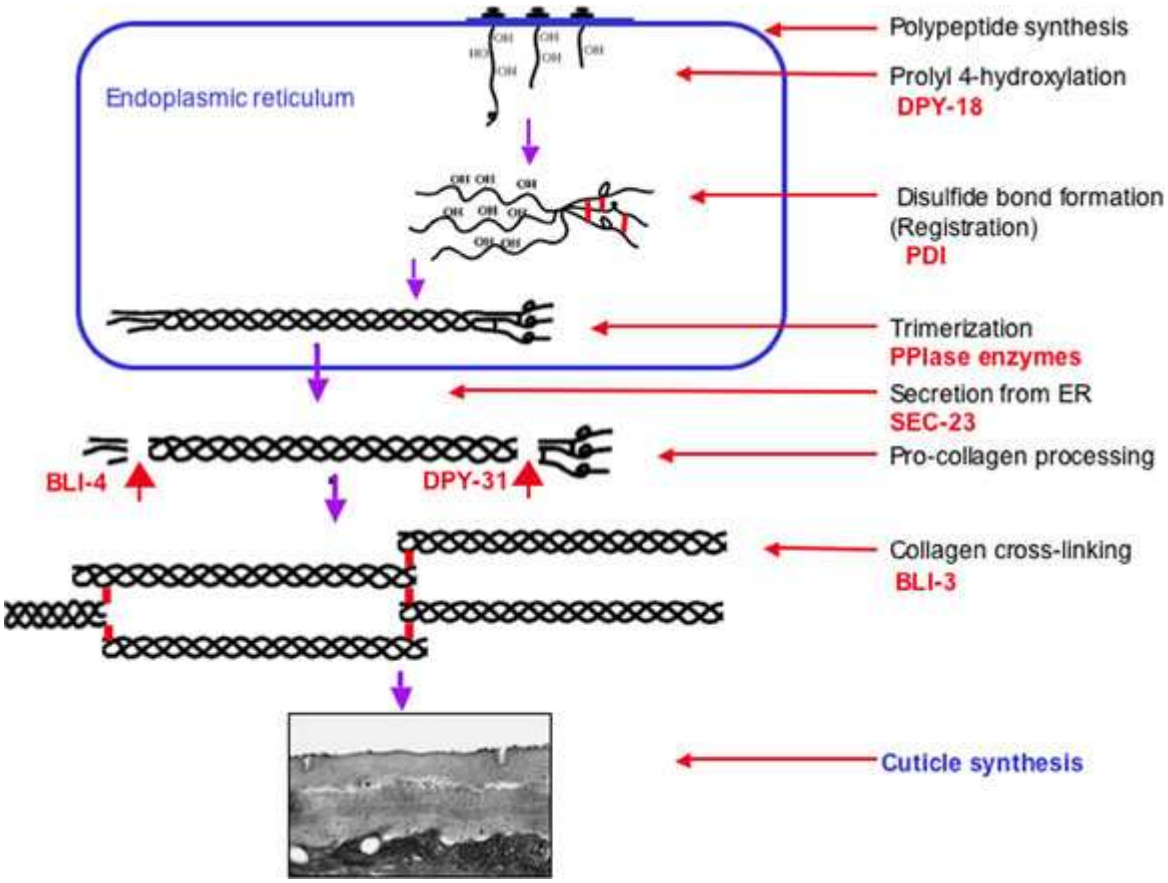

Fig. 6. Collagen biosynthesis pathway (http://www.wormbook.org/chapters/www_cuticle/cuticle.html)

V. Regulation of body size

Body size is a fundamental feature of an organism critical to survival and fitness, yet the mechanisms underlying its regulation remain somewhat mysterious. Existing studies show that body size is in part genetically controlled (Oldham et al., 2000). For example, in *Drosophila*, the insulin/insulin-like growth factor 1 (IGF1) signaling pathway regulates body size (Bohni et al., 1999; Leevers et al., 1996; Neufeld and Edgar, 1998). Drosophila homozygous for *chico,* the homologue of the vertebrate *IRSs* 1-4 (insulin receptor substrate) are smaller than wild-type flies (Chen et al., 1996). Mutations in the gene that codes for *Inr (Insulin/IGF1 receptor)* affect overall growth. In *Drosophila* Salvador– Warts–Hippo (SWH) pathway also plays a major role in the regulation of tissue size. Lack of SWH pathway component (*fat, salvador, warts, expanded Hippo* and *Merlin*) activity results in overgrowth of the adult structures (Willecke et al., 2008)**.** Clones mutated for *expanded* (*ex*) and *fat* (*ft*) genes grow more rapidly (Willecke et al., 2008 and Tyler et al., 2007). Flies mutant for Drosophila *S6 kinase* (*DS6K*) and *d-Myc* also have slow growth, reduced cell size and small body size (Gallant et al., 1996; Johnston et al., 1999; Montagne et al., 1999). Drosophila homolog of the target of rapamycin (TOR) affects the growth by modulating the activity of DS6K. Mutant cells are small in size (Neufed, 2003; Oldham et al., 2000).

Body size regulation in *C. elegans*

In *C. elegans*, there are several known small body size mutants. Components of the DBL-1/TGF-β pathway play a major role in the regulation of body size. Mutations in any component of the pathway, *dbl-1* (ligand), *sma-6* (type I receptor), *daf-4* (type II receptor), *sma-2*, *sma-3*, *sma-4* (Smad transcription factors) and *sma-9* (transcription co-factor) result in smaller than wild-type body size (Estevez et al., 1993; Krishna et al., 1999; Liang et al., 2003; Savage-Dunn, 2005; Savage-Dunn et al., 2003; Savage et al., 1996; Suzuki et al., 1999). These mutants grow more slowly than wild type worms after hatching indicating postembryonic growth defects. (Patterson and Padgett, 2000; Savage-Dunn, 2001; Savage-Dunn et al. 2003 and Maduzia et al., 2005). The *dbl-1* pathway targets the hypodermis to regulate the body size. Expression of the respective signaling component in the hypodermis is sufficient to rescue the body size defects in *sma-3* (Wang et al., 2002), *sma-6* (Yoshida et al., 2001) and *daf-4* (Inoue et al., 2000). Small body size caused by defects in DBL-1 pathway can be explained by the reduced ploidy levels in the hypodermal nuclei, small cell and organ size or reduced protein levels. It has been reported that *sma-2* and *daf-4* mutants have reduce ploidy levels in their hypodermal cells compared to 10.7C in wild type worm (Flemming et al, 2000). Volumes of the hypodermis, intestine and muscle of *sma-2*, *sma-4* and *sma-6* are reduced to about half (Nagamatsu et al., 2004). Number of hypodermal and intestinal nuclei counts is not significantly different when compared with wild type (Nagamatsu et al., 2004). Seam cells in *dbl-1* pathway mutants show reduction in size similar to reduction in the body size (Wang et al., 2002).

In addition to the DBL-1/TGF-β pathway, other genes have been identified that play less critical roles in regulation of body size. One such group is genes that are expressed in sensory neurons, including *che-2*, *che-3*, *egl-4*, *tax-6* and *cnb-1* (Bandyopadhyay et al., 2002; Fujiwara et

al., 2002; Kuhara et al., 2002). The *che-2* and *che-3* mutations cause small body size due to defects in sensory perception. *egl-4* (cGMP-Dependent Protein Kinase) acts downstream of *che* mutants to regulate body size by repressing the DBL-1 pathway (Fujiwara et al., 2002). *tax-6* and *cnb-1* encode the catalytic and regulatory subunits of calcineurin, respectively. *tax-6* interacts with *kin-29* (ser/thr kinase) and *mef-2* (MADS box transcription factor) to regulate body size (Singaravelu et al., 2007).

Mutants with feeding difficulties also have a small body size. These include *pha-2* and *pha-3* with abnormal pharyngeal anatomy, *eat-1, eat-2, eat-3* with reduced pumping rates and *eat-10* with inefficient pharyngeal pumping (Morck and Pilon, 2006). Mutations of components of TORC2 complex result in small body size (Jones et al., 2009; Soukas et al., 2009). In addition, intriguing recent evidence implicates the cell death machinery in the regulation of cell and body size (Chen et al., 2008). *sma-1* (βH-spectrin), mutants show defects in embryonic elongation. Embryonic elongation is dependent on the actin cytoskeleton. Contraction in actin fibers present in the apical plasma membrane in the epidermis causes change in the shape of the epithelial cells which leads to embryo elongation. SMA-1 could be involving stabilization of the actin cytoskeleton or it may be an intermediate molecule between actin cytoskeleton and the plasma membrane. In both situations, disruption of SMA-1 would reduce the contractile force by actin cytoskeleton (McKeown et al., 1998). *sma-5* (MAP kinase BMK1/ERK5 homolog) on the other hand controls cell growth by acting in MAP kinase pathway to regulate the body size **(**Watanabe et al., 2005).

Mutations that affect the structure of the cuticle can change the body size of the animal because the cuticle encapsulates the body. Some examples are *dpy-2*, *dpy-7*, *dpy-10, dpy-13*, *sqt-1*, *sqt-3* and *lon-3.* All of these genes encode cuticular collagens (Johnstone et al., 1992; Kramer,

1994; Kramer and Johnson, 1993; Kramer et al., 1988; Levy et al., 1993; Nystrom et al., 2002; Suzuki et al., 2002; van der Keyl et al., 1994; von Mende et al., 1988). Dpy phenotype in *dpy-5(e61)* and *dpy-11(e224)*mutants are associated with failure of the circumferential contractions in the lateral cuticle and also associated with branching or bifurcated alae. *dpy-4*, *dpy-5* and *dpy-13* mutants have closely located annuli which explain longitudinal contractions in the cuticle that results in short body length when compared to wild type (Thein et al., 2003).

ADT-2 in body size regulation

To understand the genetic basis of body size regulation, a forward genetic screen for small body size mutants was carried out (Savage-Dunn et al., 2003). In that screen, alleles of many of these genes were identified. Furthermore, one of the novel small body size mutants isolated was *sma-21*. In my thesis work, I have shown that *sma-21* encodes a metalloprotease that belongs to the ADAMTS (a disintegrin and metalloprotease with thrombospondin motifs) family.

VI. Zinc metalloproteases

Proteases that require zinc for their catalytic activity are called zinc metalloproteases. Classification of these proteases is based on the amino acid sequence around the metal binding motif in the catalytic domain (Figure 7). Four subfamilies of zinc metalloproteases, Metzincins, Inuzincin, Gluzincin and Carboxypeptidase constitute the superfamily Zincins (Jarriault and Greenwald, 2005). Superfamily Zincins include metalloproteases that have HExxH Zinc binding motif where two histidines are needed for zinc binding. Metzincins have extended zinc binding motif and methionin downstream of the zinc binding motif HExxHxxGxxHxxxxxxxM. Metzincins consists of four distinct families, the astacins, the serralysins, the matrix metalloproteases and the reprolysins (Stocker et al., 1995). Most importantly, reprolysins were originally found in snake venom and they have Asp after the third histidine in their metal binding motif. Family reprolysins contains two subfamilies; ADAM (a disintegrin and metalloprotease) and ADAMTS (a disintegrin and metalloprotease with thrombospondin motifs). ADAMs are transmembrane proteins and ADAMTSs are extracellular matrix proteins (Tang, 2001; Kuno et al., 1997).

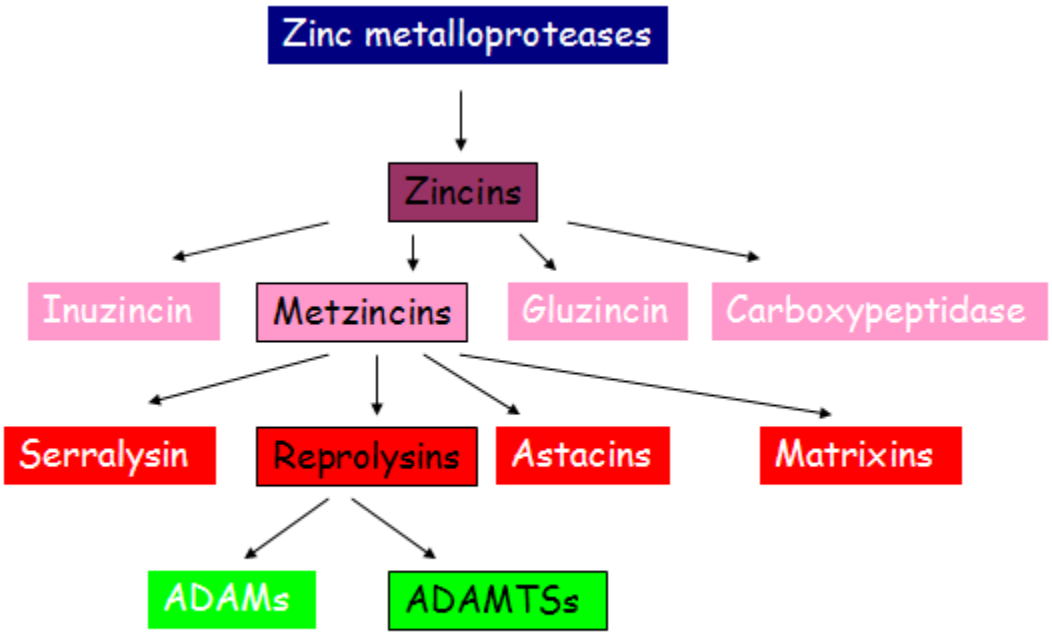

Figure 7: Classification of Zn metalloproteases

VII. Family ADAMTS (a disintegrin and metalloprotease with thrombospondin motifs)

ADAMTS are secreted metalloproteases that bind to the extracellular matrix (ECM) (Kuno and Matsushima, 1998; Porter et al., 2005; Tang, 2001). ADAMTS are related to the ADAM (a disintegrin and metalloprotease) subfamily of transmembrane proteins which plays a major role in cleaving of cell surface molecules (Porter et al., 2005). ADAMTS has several domains (Figure 8). From the N- to the C-terminus, these domains includes: (i) a signal sequence; (ii) a pro-peptide; (iii) a metalloproteinase or the catalytic domain, (iv) a disintegrin-like domain; (v) a central TS (thrombospondin type I-like) repeat; (vi) a cysteine-rich region; (vii) a spacer region ; and (viii) several number of C-terminal TS repeats. The catalytic domain has a reprolysin- type zinc-binding motif, HEX1X2HX3X1GX1XHD [where X1 is typically hydrophobic aa, X2 is glycine or a hydrophobic aa and X3 is asparagine (http://www.lerner.ccf.org/bme/apte/adamts/domain_organization.php). There is a conserved methionine residue downstream of the zinc binding motif. Three histidine and downstream methionine are important to hold the metal ion and the water molecule which is necessary for proteolytic cleavage of the substrate. Disintegrin domain shows similarity to the snake venom disintrigrins. These proteins interact with integrin receptors in platelets (Seals and Courtneidge, 2003). However, there is no evidence that ADAMTSs interact with integrins. Thrombospondin type 1-like repeats (TSR) show homology to the type I repeats present in thrombospondins 1 and 2 (Bornstein P, 1992). TS repeats and the spacer region involved in ECM binding and substrate specificity (Hashimoto,et al, 2004; Rodr´ıguez-Manzaneque, et a;, 2000; Luque, et al., 2003; Tortorella, et al., 2000; Kuno et al., 1997) .

.

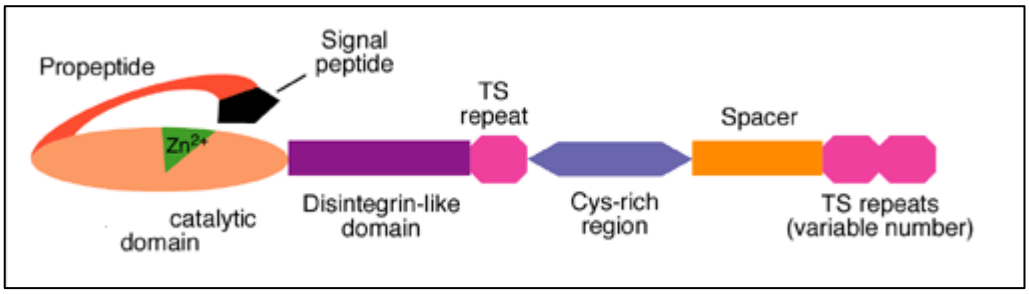

Figure 8: Domain structure of ADAMTS (Graham Riley, 2005)

VIII. ADAMTS in *C. elegans*

In *C. elegans* there are 5 ADAMTSs: GON-1, ADT-2, ADT-1, MIG-17 and T19D2.1. These ADAMTSs are involved in organogenesis. GON-1 is expressed in muscles and distal tip cell and secreted to the basement membrane of the gonad. Mutants show defects in gonadal arm elongation with a severely deformed somatic gonad. It is proposed that GON-1 remodels the basement membrane either by degrading components of the extracellular matrix (basement membrane) or by cleaving the signaling molecules or growth regulators needed for distal cell migration and somatic gonad formation (Hesselson et al., 2004; Blelloch and Kimble, 1999).

MIG-17 is also involved in distal tip cell migration in gonad development. It is expressed in body wall muscles and secreted to the basement membrane of the gonad to regulate the migration of DTC (Kimble and White, 1981; Nishiwaki et al., 2000; Kubota et al., 2008). It has been shown recently that MIG-17 recruits a basement membrane protein, nidogen, to the basement membrane to control DTC migration. This depends on two downstream proteins; fubulin-1(FBL-1) and type IV collagen LET-2 (Kubota et al., 2008).

ADT-1 plays a role in male tail ray morphogenesis. It is proposed that ADT-1 is secreted to the cuticle from the hypodermal cells in the male tale in order to remodel the ECM (cuticle) in ray morphogenesis (Kuno et al., 2002).

IX. Biological role of mammalian ADAMTS

In mammals ADAMTS play a major role in extracellular matrix assembly and degradation. Procollagen N-proteinases: ADAMTS-2, -3 and -14 are involved in ECM assembly. Procollagen N-proteinases remove the N-propeptide of the procollagen which is necessary for the proper assembly of collagen into fibrils. Aggrecanases: ADAMTS-1, -4, -5, -8, -9 and -15 are involved in ECM degradation (Colige et al., 1995; Colige et al., 1997; Collins-Racie et al., 2004; Fernandes et al., 2001; Kuno et al., 2000; Somerville et al., 2003; Tortorella et al., 2000; Tortorella et al., 2005; Wang et al., 2003). Aggrecan is the major proteoglycan present in the cartilage. It has been shown that ADAMTS-4,-5 cleave aggrecan at Glu373-Ala374 and several other sites. Degradation of aggrecan will lead to loss of compressive properties of cartilage which finally lead to arthritis (Arner, 2002). ADAMTS-1 and -4 can also process two other types of proteoglycan such as versican and brevican (Porter et al., 2005). ADAMTS-1 plays a role in angiogenesis. ADAMTS-13 cleave plasma von Willebrand factor (VWF). This factor is involved in platelet aggregation. ADAMTS-13 also mediates adhesion of the platelets to the collagen/ECM during vascular damage (Brass, 2001).

ADAMTS function is also relevant to human diseases and disorders. *ADAMTS2* is associated with connective tissue disorders such as EDS (Ehlers-Danlos syndrome) in humans, and with dermatosparaxis in cattle. Both disorders are characterized by fragility of skin and short stature (Colige et al., 1999; Lenaers et al., 1971). Mutations in *ADAMTS13* cause inherited thrombocytopenic purpura (TTP), a disorder of blood coagulation (Levy et al., 2001). A

mutation in *ADAMTS10* is associated with Weill-Marchesani syndrome (WMS), a disorder that is characterized by short body size, short fingers and toes, joint stiffness and eye anomalies (Dagoneau et al., 2004). Genome wide studies have identified variants associated with human height located at or nearby genes involved in skeletal development including *ADAMTS17*, *ADAMTS10*, *ADAMTS3* and *ADAMTSL3* (Gudbjartsson et al., 2008; Lettre et al., 2008; Weedon et al., 2008).

Chapter 1. *sma-21*, a gene required for normal body size in *C. elegans*, encodes ADT-2 ADAMTS secreted metalloprotease.

INTRODUCTION:

Organismal growth and body size are influenced by both genetic and environmental factors. We have utilized the strong molecular genetic techniques available in the nematode *C. elegans* to identify genetic determinants of body size. In *C. elegans*, DBL-1, a member of the conserved family of secreted growth factors known as the Transforming Growth Factor β superfamily, is known to play a major role in growth control. The mechanisms by which other determinants of body size function, however, are less well understood. Therefore, identification of new determinant of body size will provide the better understanding of existing and new pathways. In order to achieve this, a forward genetic screen for small body size mutants was carried out (Savage-Dunn et al., 2003). In that screen, alleles of many genes in the DBL-1 pathway were identified. Furthermore, one of the novel small body size mutants isolated was *sma-21*, which we now show is allelic with ADAMTS family member *adt-2*.

ADAMTS (a disintegrin-like and metalloprotease with thrombospondin type I motif) are secreted metalloproteases that bind to the extracellular matrix (ECM) (Kuno and Matsushima, 1998; Porter et al., 2005; Tang, 2001). ADAMTS are related to the ADAM (a disintegrin and metalloprotease) subfamily of transmembrane proteins. Both ADAM and ADAMTS are Zn dependent metalloproteases (Jones and Riley, 2005; Kaushal and Shah, 2000; Stocker et al., 1995). These proteins are multidomain with multiple functions. In mammals, the ADAMTS proteases are believed to function in ECM assembly (procollagen N-proteinases: ADAMTS-2, -3 and -14) and ECM degradation (aggrecanases: ADAMTS-1, -4, -5, -8, -9 and -15) (Colige et al., 1995; Colige et al., 1997; Collins-Racie et al., 2004; Fernandes et al., 2001; Kuno et al., 2000; Somerville et al., 2003; Tortorella et al., 2000; Tortorella et al., 2005; Wang et al., 2003). In *C.*

elegans, some of these proteases are involved in organogenesis by remodeling the ECM. For example, GON-1 and MIG-17 are involved in distal tip cell migration in gonad development (Blelloch and Kimble, 1999; Ihara and Nishiwaki, 2007). Another protease ADT-1 is involved in ray morphogenesis by rapid remodeling of ECM (Kuno et al., 2002). In this chapter I will discuss the detailed phenotypic characterization and molecular cloning of *sma-21*.

MATERIALS AND METHODS

Strains

C. elegans strains were grown at 20^0C using standard methods (Brenner, 1974). In addition to strains generated in this study the following strains were used:

N2 and HA (wild type)

LG V: *dbl-1(wk70)*

adt-2(tm975) obtained from Dr. Shohei Mitani, National Bioresource Project for the nematode, Tokyo Women's Medical University School of Medicine, Japan.

Transgenics: *wIs51* [SCM::GFP, *unc-119(+)*]; *jcIs1* [*ajm-1::gfp*] obtained from Dr. Jeff Simske; *arIs99* [*dpy-7*p*::2Xnls::yfp*] obtained from Dr. Iva Greenwald.

Mapping

We used SNP mapping (Davis et al., 2005) to locate the *sma-21* gene on the X chromosome. HA males were crossed into *sma-21* hermaphrodites. From the resulting heterozygous worms, 30-50 homozygous mutant (homozygous for N2 DNA surrounding the mutation) worms and phenotypically non mutant worms (heterozygous for N2/HA or homozygous for HA/HA) were picked. Worm lysates from these two groups were used to do PCR with 48 pairs of primers that flank SNPs covering the whole genome of the *C. elegans*. After amplification, PCR products were digested with *Dra*I and bands were analyzed to determine the linkage. After determining the linkage group and the approximate position of the mutation, interval mapping was done to further narrow down the region of *sma-21*. HA males were crossed into *sma-21* hermaphrodites. From the progeny of the heterozygotes, about 50-70 mutants were segregated into separate plates. Worm lysates from the F3 progeny worms were used to do a PCR using the SNP primers

on the X chromosome. After amplification, PCR product was digested using *DraI* and banding patterns were analyzed.

Molecular cloning and sequencing of *sma-21*

The region of *sma-21* was narrowed down to about 0.6 MB and we then employed aCGH (Maydan et al., 2009) as previously described. This work was done in collaboration with Dr. Donald Moreman at University of British Columbia. Briefly, a microarray was designed for a 0.6 MB region delimited by the standard SNP mapping protocol using an application at http://hokkaido.bcgsc.ca/SNPdetection/. Processing of the microarray was done by Roche/NimbleGen. To confirm the polymorphisms identified by aCGH, we generated PCR fragments flanking the mutation sites and directly sequenced them.

5’ adt-2-F6: 5’ ACCAGACAACCGGTAGGGATG 3’

3’ adt-2 –R6: 5’ CCCTTCTATGTGTTCCCAATT 3’

5’ K09f5.1 – F2: 5’ GGAGGTGGTGTTGTCAATTCA 3’

3’ K09f5.1 – R2 5’ ATCTGAAAACTTGAATAGTGA 3’

The PCR amplification produces 752 bp fragment for the wild-type allele and a 277 bp fragment for the deletion allele.

Deletion in *adt-2(tm975)* was confirmed by using following primers.

5’ adt-2 F1: 5’ AATCACGGAAACGCTCAAATGTAC 3’

3’ adt-2 R1: 5’ CGGGTTTCACATTGGACGAGATTT 3’

For rescue, 10 ng/µl fosmid DNA was injected into the gonadal syncytia of *sma-21(wk156)* hermaphrodites with myo-3::mcherry (kindly provided by Dr. Hannes Bülow) as a marker (Mello et al., 1991). Total concentration of the DNA at injection was adjusted to 100 ng/µg using Bluescript SK. yk cDNAs spanning this region were obtained from Dr. Y. Kohara. The yk1586e04 was sequenced and the predicted transcript structure was verified. Primers used for sequencing:

Adt-2 F2- 5'caa ctc tcg caa agt tgc tct 3'

Adt-2 F7 – 5' cca agc ata tca tgt cat cat 3'

Adt-2 F11 – 5' aat cac tga cca atc gtc gtc 3'

Adt-2 F13- 5' gtg tag tga aac atg tgg cga cgg 3'

Adt-2 F14 5' agc atg tgc ttc gtc aag tgc aaa 3'

Adt-2 R 14- 5'gat gat aat atg gta ctg gat caa 3'

Adt-2 R7 – 5' cca ata gcg tta cag gga cca 3'

Adt-2 R8 5' acc cgt agt tat gag gcg acc agt 3'

Adt-2 R 15- 5' atc cgt ttc cat gca tca att cgc 3'

pME18Fw2 - 5' tca gtg gat gtt gcc ttt ac 3'

Me1250RV - 5' tgt ggg agg ttt ttt ctc ta 3'

Measurement of nuclear and cell numbers

We counted the number of nuclei in the hypodermis, seam cells and intestine in wild-type and *adt-2* mutant animals. DAPI staining was used to label the intestinal nuclei. N2, *adt-2* worms were fixed with acetone, washed with PMB and immersed in 500 µl/ml DAPI solution for 30

minutes. Worms were then washed twice with PMB and the intestinal nuclei were counted. The number of seam cell nuclei was counted using the transgene *wIs51* [SCM::GFP, *unc-119(+)*], a seam cell marker in adult animals. The number of nuclei in the hypodermis of L4 animals was counted using the transgene *arIs99* [*dpy-7*p*::2Xnls::yfp*], a hypodermal reporter, which is expressed in hyp7 and other hypodermal cells (Myers and Greenwald, 2005). Seam cell perimeter was measured in L3 larvae using the *ajm-1::gfp* marker (Mohler et al., 1998) which localizes to adherens junctions. The length of the pharynx and the body size of the same L3 worms were also measured. These markers were introduced into *adt-2(wk156)* by standard genetic crosses. Images were taken using a confocal or epifluorescence microscope.

RNAi feeding

RNAi feeding was performed as described in (Kamath et al., 2001). Six L4 animals were transferred to feeding plates, incubated overnight, transferred to fresh plates and the progeny were scored.

Analysis of body size measurements

To characterize the body size phenotype of *sma-21*, I created a growth curve by measuring the body lengths of wild type N2 worms and *sma-21(wk156)* at various times after embryo collection. Worms were grown at 20^0C and photographed using Axio Vision 3.00 software. The length of each worm was determined by drawing a segmented line along the midline using the same software.

Lifespan assay

Synchronous animals were obtained by bleaching of gravid hermaphrodites. 120 L4 worms from wild type, *adt-2(wk156)* and *adt-2(RNAi)* were picked. Adult N2 worms also treated with *adt-2* RNAi were tested for their lifespan. From each strain, the L4 worms were divided into 12 plates with 10 worms per plate. Worms were transferred to fresh plates every other day and the number of surviving worms was counted. Worms were marked as dead if they failed to respond to the nose tap with a platinum wire.

RESULTS

1. Isolation and mapping of *sma-21* mutants.

To identify genes required for body size regulation, a forward genetic screen for small body size mutants was carried out (Savage-Dunn et al. 2003). In that screen, N2 hermaphrodites were mutagenized with ethyl methanesulfonate (EMS) and the F2 progeny worms were screened for small body phenotype. In the screen, *sma-20* mutants were identified. In the course of mapping, we found out that the *sma-20* strain has two mutations, *sma-20(wk31)* and *sma-21(wk156)*. Furthermore, 23 semi-small segregants were isolated from the double mutant strain and it was found that they were all allelic to *sma-21*. This finding led us to the conclusion that *sma-21* regulates body size, and it is believed that *sma-20* is an enhancer of the *sma-21* phenotype with no apparent phenotype on its own.

A single nucleotide polymorphism (SNP) mapping (Davis et al., 2005) was used to find the linkage group of *sma-21*(Fig. 9A). SNPs exist in HA and N2 backgrounds. Heterozygous progeny from a cross between *sma-21*(isolated in N2 background) hermaphrodites and HA males were singled into separate plates. Pooled worm lysates from about 30-50 small and non small worms of the F2 generation were used for the PCR with 48 pairs of SNP primers, which cover the whole *C. elegans* genome. *sma-21* shows clear linkage to the chromosome X (Fig. 9B). Linkage is visible as a decrease in the proportion of HA DNA in *sma-21* lanes when compared to the wild-type lanes in the chromosome X. *sma-21* does not show linkage to any other chromosome. For example, results from the linkage group III are shown. Proportion of HA and *sma-21* DNA is not different (Fig 9C). Once the linkage group of the *sma-21* was determined, interval mapping was done to narrow down the region of the *sma-21*. In the interval mapping, small and non small F2 progeny from the heterozygote (*sma-21*/HA) were singled out into

separate plates. Worm lysates from each plate were used for the PCR analysis. Table 1 shows the results of the interval mapping. Based on the data, *sma-21* was placed between – 1.7 to - 0.7 map units on the X chromosome.

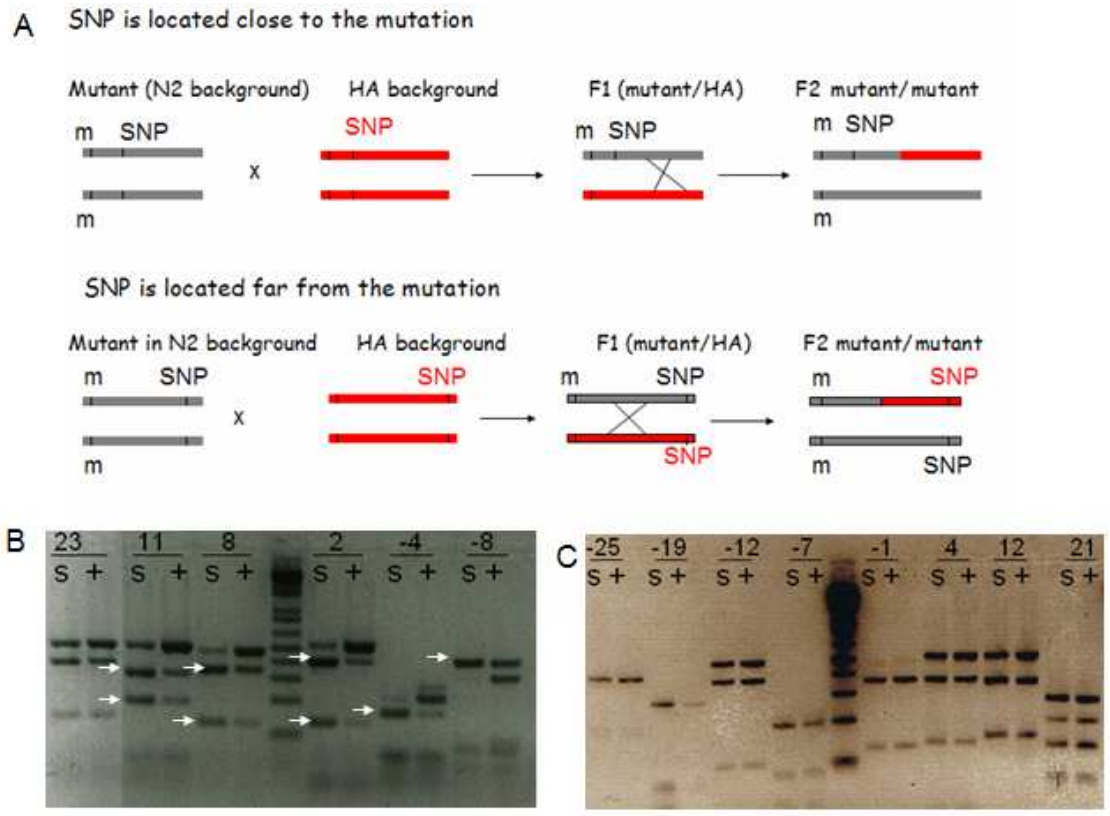

Figure 9. SNP mapping. A) When the SNP is located close to the mutation, most likely the crossing over will take place in the region to the right of the SNP. The result will be strong N2 bands in the mutant lanes. When the mutation lies far from the SNP, most likely the crossing over will take place between the SNP and the mutant resulting N2 and HA bands with equal strength. (Gray –N2 background; red – HA background; m – mutant gene). B) *sma-21* is linked to the chromosome X. Each pair of lanes shows the results from the SNP at the indicated genetic map position, using either the *sma-21*(S) or the HA (+) worm lysate. Linkage is visible as a decrease in the proportion of HA DNA and an increase of N2 DNA in *sma-21* lanes (S, white arrows) compared to the wild-type lanes (+) in LG X. C) *sma-21* is unlinked to the linkage group III. Proportion of HA(+) and N2(S) DNA is similar.

Table 1: SNP Interval mapping

SNP and the genetic map position	Number of recombinant with HA band
F49H12 (-17)	45/45
ZK470 (-8)	12/67
C46F4 (-4)	6/67
C01C10 (-1.7)	1
CE6 (-1)	None
F45E1 (-0.7)	3/67
F11A1 (2)	9/67
F22E10 (8)	9/39

2. *sma-21* encodes a ADAMTS (disintegrin and metalloprotease with thrombospondin repeats) family member ADT-2

Single nucleotide polymorphism (SNP) mapping (Davis et al., 2005) placed *sma-21* on the X chromosome in the region between 7,439,984 (cosmid C01C10) and 7,982,355 (cosmid F45E1). array comparative genomic hybridization (aCGH) was done in collaboration with Dr. Donald Moerman at University of British Columbia to identify any polymorphisms in this region. An oligonucleotide chip spanning this region was designed. This was hybridized with *sma-21* and wild-type genomic DNA at Roche NimbleGen (Maydan et al., 2009). This analysis identified two polymorphisms in *sma-21*: one in K09F5.1 and one in *adt-2*. Sequence analysis of PCR fragments in *sma-21* verified the two SNPs: one at 7590038 bp (G to A) in *adt-2* gene and the other at 7740620 (G to A) in K09F5.1. To determine which of these mutations is responsible for small body size in *sma-21*, we used RNAi and transformation rescue. We inactivated the corresponding genes by feeding N2 (wild type) and *rrf-3* (RNAi hypersensitive) worms on *adt-2* RNAi and K09F5.1 RNAi plates (Kamath et al., 2001). *adt-2* RNAi fed worms were small unlike the K09F5.1 RNAi (Fig. 10). Then, we introduced fosmid clones containing *adt-2* wild-type sequence into *sma-21* mutants by microinjection (Mello et al., 1991). Fosmid clone (WRM0636aH08) which contains the full length *adt-2* wild-type gene, rescues the body size of *sma-21(wk156)* (Fig. 10). Finally, we performed a complementation test between *sma-21* and a deletion allele of *adt-2*(*tm975*) obtained from the CGC, and determined lack of complementation. The test shows that these two mutations do not complement. Putting all the data together, we can conclude that *sma-21* encodes ADT-2.

In order to verify exon-intron structure of *adt-2,* we sequenced the cDNA clones obtained from Dr Yuji Kohara. Sequence of EST yk1586e04 containing the full length of the transcript

reveals *adt-2* consists of 20 exons (exon 1 is non-coding) that encode a protein of 1020 amino acids. ADT-2 belongs to ADAMTS family of secreted extracellular metalloproteases. As shown in Table 2, the catalytic domain of ADT-2 shows 21% to 41% homology to other ADAMTS family members. These proteins bind to extracellular matrix (ECM) and are believed to be involved in remodeling of the ECM (Porter et al., 2005). This family of proteins comprise of several domains. Starting with the N- terminus, ADT-2 has a signal peptide predicted by SignalP 3.0 Server; a catalytic domain with a reprolysin- type zinc-binding motif, HEX1X2HX3X1GX1XHD [where X1 is typically hydrophobic aa, X2 is glycine or a hydrophobic aa and X3 is asparagine (http://www.lerner.ccf.org/bme/apte/adamts/domain_organization.php)], cysteine-rich; a central TS (thrombospondin type I-like) and six C- terminal TS repeats predicted by SBASE release 14, Sept 2006 (Fig. 11A). Domain organization of mammalian ADAMTS-2 is shown for comparison (Fig. 11A). Table 2 shows the amino acid identity in the zinc binding motif, catalytic domain and in the first thrombospondin type I-like repeat of *C. elegans* ADT-2 to mammalian and *C. elegans* ADAMTS. The metalloprotease domain of ADT-2 shows the highest similarity to ADAMTS-2, -3, and -14 among mammalian ADAMTS family members (Table 2 and Fig. 11D).

adt-2(wk156) is a missense mutation that changes one of the conserved glycine residues to a serine (highlighted in red in Fig. 11C), within the metal binding motif. Conservation of this glycine residue suggests that it is functionally important. *adt-2*(*tm975)* has a deletion of 475bp (wormbase; Fig. 11B) which deletes 92 amino acids within the catalytic domain including the metal binding motif. *adt-2(tm975)* is lethal. Homozygous *adt-2(tm975)* mutant animals die during embryogenesis, at the 3-fold stage or during hatching (Fig. 12B and C).

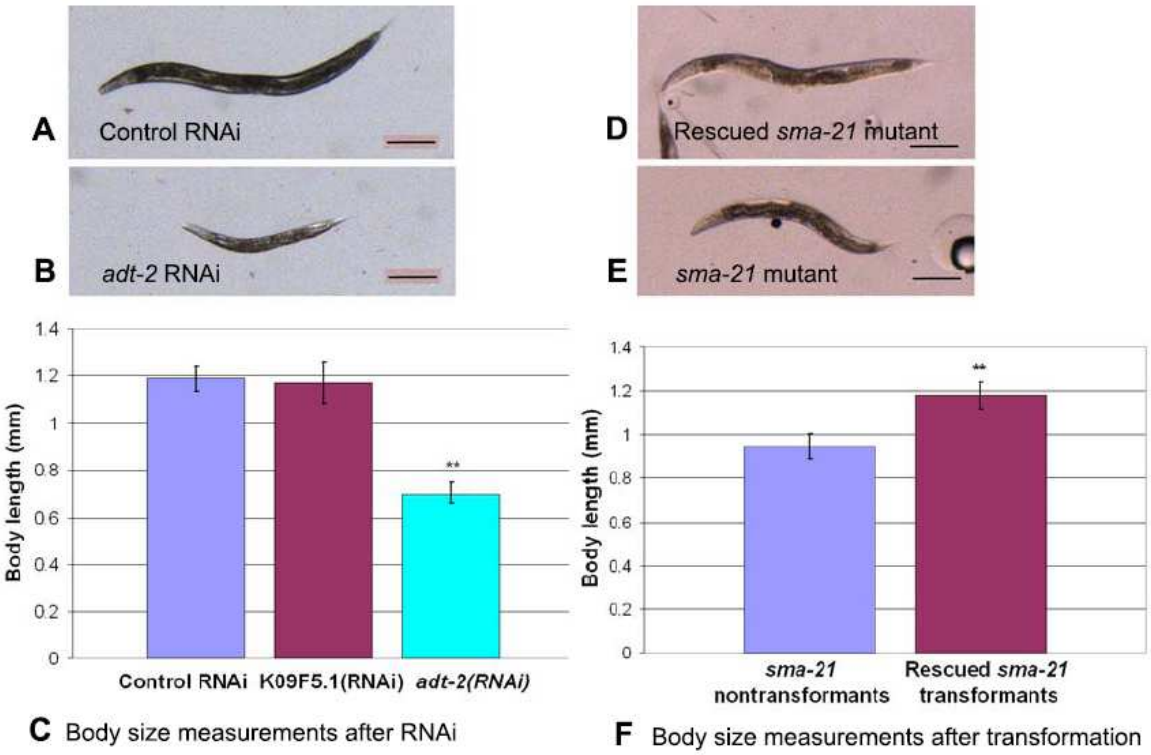

Figure 10. *sma-21* encodes ADT-2. (A,B,C) RNAi inactivation of *adt-2* results in small body size. K09F5.1(RNAi) treated worms were indistinguishable from control worms. *rrf-3* RNAi hypersensitive strain is used for body size measurements. (D,E,F) Fosmid WRM0636aH08 containing *adt-2* gene rescues the body size of *sma-21(wk156).* A,B,D and E are adult worms photographed at the same magnification. Body length was measured in adult worms. Each value represents a mean of 30 – 60 worms. Error bars indicate the standard deviation. Scale bars = 0.2mm. **indicates $p<0.01$

Fig. 11. Structure of the ADT-2 protein. (**A**) Domain organization of ADT-2 protein. Domain organization of mammalian ADAMTS-2 is shown for comparison (predicted by SBASE and SignalP 3.0 Server). (**B**) Amino acid sequence of ADT-2. Different domains are highlighted. In red is the signal sequence; in violet, the prodomain; in brown, the catalytic domain. Underlined is the Zn binding motif. In green is the conserved methionine residue downstream of the metal binding motif which forms 'Met-turn' (Porter et al., 2005). In yellow is the cysteine rich domain. Thrombospondin type I-like repeats are highlighted in blue. The location of the deletion in *tm975* and the missense mutation (Gly^{364} – Ser) in *wk156* are indicated by a shaded box and an asterisk, respectively. (**C**) Zinc binding motif and Met turn of *C. elegans* ADT-2 are aligned with other mammalian and *C. elegans* ADAMTS family members. The conserved zinc binding motif and methionine residue downstream of the metal binding site are shaded. Asterisks indicate conserved amino acids. The glycine in red is the conserved residue mutated in *adt-2(wk156).* (**D**) Phylogenetic tree showing relationships between *C. elegans* and human ADAMTS sequences (constructed using BioEdit sequence Alignment Editor and MEGA 4.0.2). The numbers above the nodes indicate the percent bootstrap values in 500 replicates of the data.

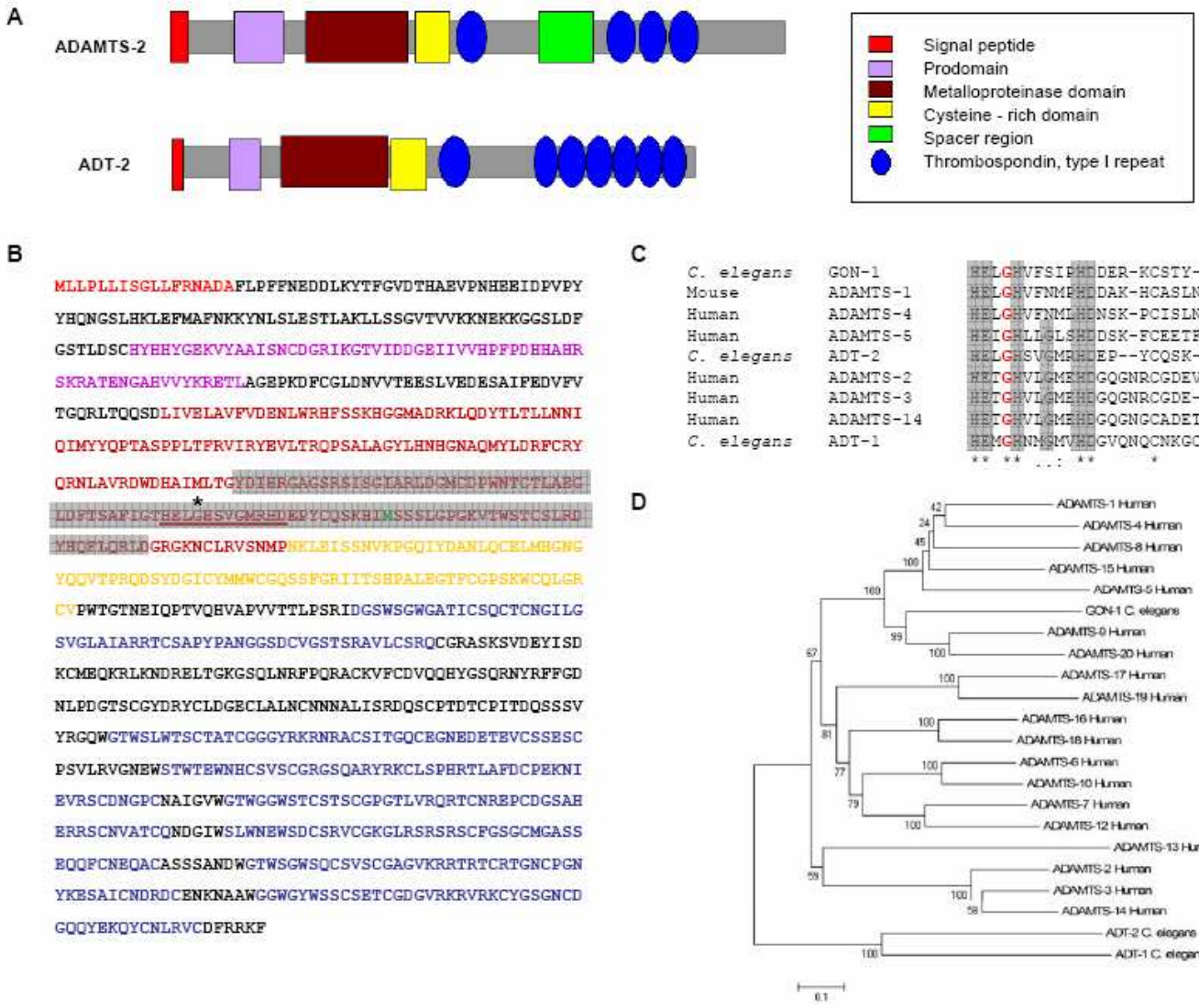
A
ADAMTS-2
ADT-2
Signal peptide
Prodomain
Metalloproteinase domain
Cysteine - rich domain
Spacer region
Thrombospondin, type I repeat
B
MLLPLLISGLLFRNADAFLPFFNEDDLKYTFGVDTHAEVPNHEEIDPVPY
YHQNGSLHKLEFMAFNKKYNLSLESTLAKLLSSGVTVVKKNEKKGGSLDF
GSTLDSCHYHHYGEKVYAAISNCDGRIKGTVIDDGEIIVVHPFPDHHAHR
SKRATENGAHVVYKRETLAGEPKDFCGLDNVVTEESLVEDESAIFEDVFV
TGQRLTQQSDLIVELAVFVDENLWRHFSSKHGGMADRKLQDYTLTLLNNI
QIMYYQPTASPPLTFRVIRYEVLTRQPSALAGYLHNHGNAQMYLDRFCRY
QRNLAVRDWDHAIMLTGYDIERCAGSRSISGIARLDVMCDPWNTGTLAEG
LDFTSAFDGTHELGHSVGMRHDEPYCQSKHIMSSSLGPGKVTWSTCSLRD
YHQFLQRLDGRGKNCLRVSNMPNKLEISSNVKPGQIYDANLQCELMHGNG
YQQVTPRQDSYDGICYMMWCGQSSFGRIITSHPALEGTPCGPSKWCQLGR
CVPWTGTNEIQPTVQHVAPVVTTLPSRIDGSWSGWGATICSQCTCNGILG
SVGLAIARRTCSAPYPANGGSDCVGSTSRAVLCSRQCGRASKSVDEYISD
KCMEQKRLKNDRELTGKGSQLNRFPQRACKVFCDVQQHYGSQRNYRFFGD
NLPDGTSCGYDRYCLDGECLALNCNNNALISRDQSCPTDTCPITDQSSSV
YRGQWGTWSLWTSCTATCGGGYRKRNRACSITGQCEGNEDETEVCSSESC
PSVLRVGNEWSTWTEWNHCSVSCGRGSQARYRKCLSPHRTLAFDCPEKNI
EVRSCDNGPCNAIGVWGTWGGWSTCSTSCGPGTLVRQRTCNREPCDGSAH
ERRSCNVATCQNDGIWSLWNEWSDCSRVCGKGLRSRSRSCFGSGCMGASS
EQQFCNEQACASSSANDWGTWSGWSQCSVSCGAGVKRRTRTCRTGNCPGN
YKESAICNDRDCENKNAAWGGWGYWSSCSETCGDGVRKRVRKCYGSGNCD
GQQYEKQYCNLRVCDFRRKF
C
C. elegans GON-1 HELGHVFSIPHDDER-KCSTY----------M 33
Mouse ADAMTS-1 HELGHVFNMPHDDAK-HCASLNGVTGDS-HLM 36
Human ADAMTS-4 HELGHVFNMLHDNSK-PCISLNGPLSTSRHVM 54
Human ADAMTS-5 HEIGHLLGLSHDDSK-FCEETFGSTEDK-RLM 31
C. elegans ADT-2 HELGHSVGMRHDEP--YCQSK--------HIM
Human ADAMTS-2 HETGHVLGMEHDGQGNRCGDEVRLG----SIM 36
Human ADAMTS-3 HETGHVLGMEHDGQGNRCGDE--------TAM 36
Human ADAMTS-14 HETGHVLGMEHDGQGNGCADETSLG----SVM 36
C. elegans ADT-1 HEMGHNMGMVHDGVQNQCNKGCCL-------M 36
D
ADAMTS-1 Human
ADAMTS-4 Human
ADAMTS-8 Human
ADAMTS-15 Human
ADAMTS-5 Human
GON-1 C. elegans
ADAMTS-9 Human
ADAMTS-20 Human
ADAMTS-17 Human
ADAMTS-19 Human
ADAMTS-16 Human
ADAMTS-18 Human
ADAMTS-6 Human
ADAMTS-10 Human
ADAMTS-7 Human
ADAMTS-12 Human
ADAMTS-13 Human
ADAMTS-2 Human
ADAMTS-3 Human
ADAMTS-14 Human
ADT-2 C. elegans
ADT-1 C. elegans
0.1

Table 2. Amino acid identity of *C. elegans* of ADT-2 to mammalian and *C. elegans* ADAMTS (calculated using Clustalw)

	Catalytic domain	First TSP type 1 motif	Zn binding motif
C. elegans ADT-1	41	37	36
C. elegans GON-1	26	35	33
Human ADAMTS-2	29	37	36
Human ADAMTS-3	26	35	36
Human ADAMTS-4	25	33	54
Human ADAMTS-14	25	32	36
Human ADAMTS-5	22	32	31
Mouse ADAMTS-1	21	33	36

3. adt-2 mutants are small in body size, and are short-lived

To characterize the body size phenotype of *adt-2(wk156)*, we created a growth curve by measuring the body length of wild-type N2 worms and *adt-2(wk156)* worms at various times after egg collection (Fig. 12A). Newly hatched *adt-2* mutant larvae have the same body length as control animals, indicating a lack of defects in embryonic elongation. *adt-2* mutant worms grew more slowly after 24 hours resulting in adult worms with about a 20 percent reduced body length when compared to wild-type. Interestingly, adult *adt-2* mutants show a significant decrease in body length between 96 and 120 hours, whereas wild-type animals continue to grow larger during adulthood. The reduction in body length in *adt-2* mutants suggests that the gene is required for maintenance of body length as well as for increase in body length during growth stages.

Next, I evaluated the effects on lifespan by *adt-2* mutants. *adt-2(wk156)* and *adt-2(RNAi)* treated worms have a significant life-span reduction compared to wild type animals (Fig. 12D). To rule out developmental defects causing early lethality, I also treated N2 animal with *adt-2 (RNAi)* starting in adulthood. These worms also show a reduction in the life span compared to wild type animals.

Figure 12. Phenotypes of *adt-2* mutants. (**A**) *adt-2(wk156)* mutant has small body size. Growth curve of *adt-2* showing reduced growth rate compared to wild-type N2 worms. Each time point represents a mean of 25-50 animals. Error bars indicate the standard deviation. Body size of *adt-2* mutant at each point except 24 hrs is significantly different from that of wild-type. (**B,C**) Lethal phenotype of *adt-2(tm975)* deletion homozygotes. Images show an unhatched embryo (three-fold stage; B) and a partially hatched larva. D) Reduced life span of *adt-2* mutants (n=120 worms).

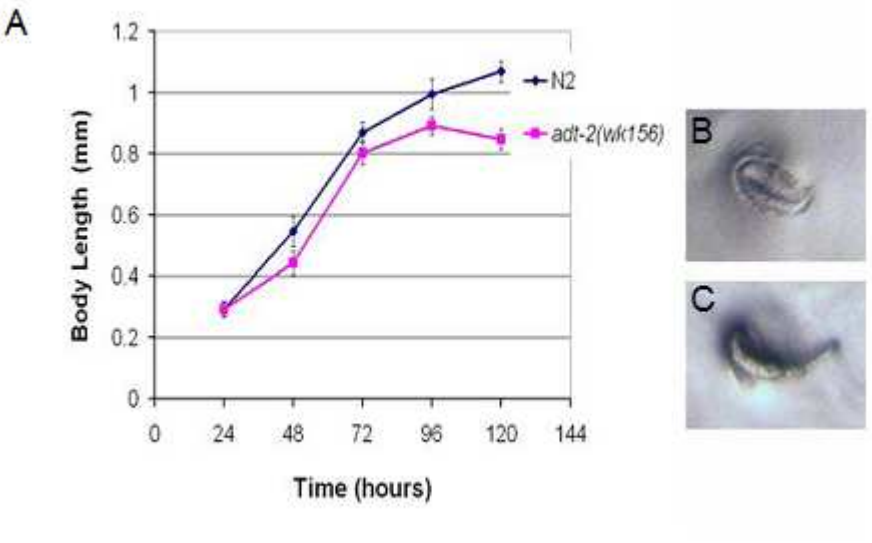
A
1.2
1
0.8
0.6
0.4
0.2
0
Body Length (mm)
0
24
48
72
96
120
144
Time (hours)
N2
adt-2(wk156)
B
C

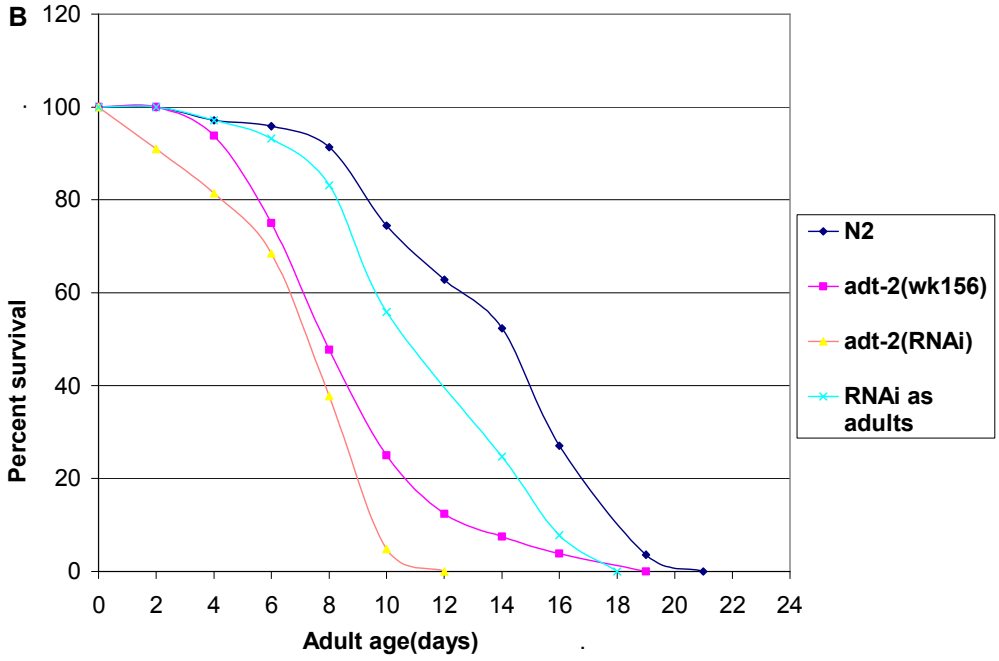
B
120
100
80
60
40
20
0
Percent survival
0
2
4
6
8
10
12
14
16
18
20
22
24
Adult age(days)
N2
adt-2(wk156)
adt-2(RNAi)
RNAi as adults

4. *adt-2* mutants have the same number of seam cells, hypodermal and intestinal cells but the seam cell size is reduced.

Reduction of body length could be due to decreased cell number, cell size or both. In order to determine which cause is responsible in this case, we first examined the number of hypodermal nuclei, the number of seam cells, and the number of intestinal cells in wild-type and *adt-2* mutant animals. The number of seam cells was measured using the *seam cell marker::GFP* and found to be not significantly different in *adt-2* compared to that of wild-type (Table 3 and Fig. 13A). We also counted the number of nuclei in the hypodermis of L4 worms, intestine, and in the seam of adult *adt-2* and *dbl-1* mutants and in wild type worms. Hypodermal nuclei were counted using *dpy-7*p*::2Xnls::yfp* marker, (Fig. 13B) which is expressed in hyp7, and other hypodermal cells, beginning at the L1 stage (Myers and Greenwald, 2005). Images were taken using a confocal microscope that provides the advantage of reconstruction of three dimensional images from several thin sections of the worm. DAPI staining was also done in order to count intestinal nuclei (Fig. 13C). The number of hypodermal nuclei, as well as intestinal and seam cells, are not significantly different in *adt-2* compared to that of wild-type (Table 3). The number of hypodermal nuclei in *dbl-1* is also not significantly different from wild type (114.6 +/- 9.4 in *dbl-1* and Table 3).

We also measured the length of two accessible tissues (seam cells and the pharynx) in *adt-2* and wild type. We crossed *ajm-1::gfp* seam cell marker into *adt-2(wk156)* and fluorescence was observed in the L3 larval stage. The *ajm-1:: gfp* marker localizes at the adherens junctions in the seam cells (Fig. 13D) (Mohler et al., 1998). The body length and pharynx length of the same L3 worms were also measured. The body length and seam cell perimeter are reduced

significantly in *adt-2* mutants compared to wild-type animals, but the length of the pharynx was not affected (Table 3). The data are consistent with the hypothesis that *sma-21* mutants are smaller at least partly due to decreased cell size, rather than decreased cell number. These defects are similar to those seen in mutants of the DBL-1 signaling pathway (Wang et al., 2002).

Fig 13. Cell size not the cell number is reduced in *adt-2* mutants A) Localization of seam cell marker::GFP in Seam cell nuclei in *adt-2(wk156).* B) Localization of *dpy-7::YFP* in hypodermal nuclei in *adt-2(wk156).* C) DAPI (4 ,6-diamidino-2-phenylindole) staining of intestinal nuclei (arrows). D) Localization of *ajm-1::gfp at* adherens junctions in wild type worms (asterisk).

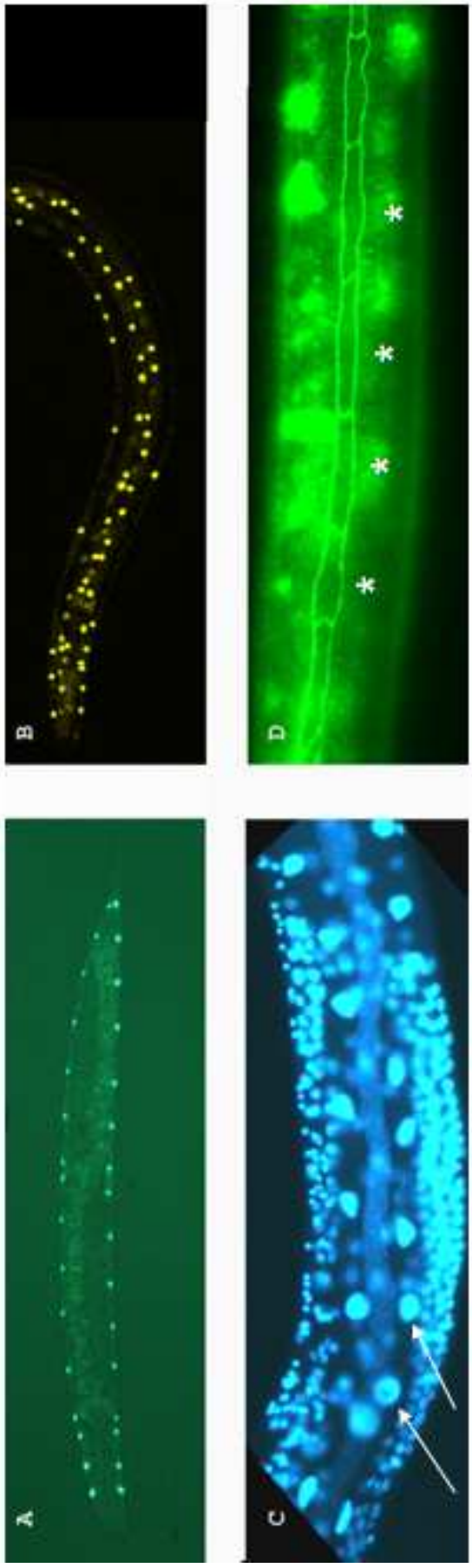
B
D
A
C

Table 3. Cell and nuclei numbers of the *adt-2(wk156)* and wild-type worms

	N2	***adt-2(wk156)***
Body size (L3) (mm)	**0.651 +/- 0.053 (n=23)**	**0.575 +/- 0.065 (n=27) ****
Seam cell perimeter (L3) (mm)	**0.073 +/- 0.011 (n=78)**	**0.067 +/- 0.011 (n =76) ****
Pharynx length (L3) (mm)	**0.109 +/- 0.006 (n=18)**	**0.108 +/- 0.009 (n=18)**
Seam cell number (adult worms)	**16 (n=30)**	**16 (n=30)**
Intestinal nuclei number (adult worms)	**31.4 +/- 1.2 (n = 31)**	**31.5 +/-1.4 (n = 38)**
Hypodermal nuclei number (L4)	**116.3 +/- 11.9 (n = 33)**	**114.1 +/- 10.7 (n = 31)**

****p<0.01 compared to wild-type (N2)**

DISCUSSION

sma-21* encodes a ADAMTS family member ADT-2, a gene required for normal body size in *C. elegans.

In this study, I have shown that *sma-21* encodes an ADAMTS family gene *adt-2*. Four pieces of evidence that support this conclusion are: first, *sma-21* has a missense mutation in a conserved glycine residue in the metal binding motif of the catalytic domain; second, inactivation of *adt-2* gene by RNA interference results in small body size. Third, fosmid clone containing *adt-2* is sufficient to rescue the body size defect of *sma-21* mutants. Fourth, a lethal deletion allele of *adt-2* fails to complement *sma-21(wk156*) small body size phenotype.

adt-2 mutants exhibit series of body size and developmental defects. Partial loss of function mutant *wk156* show mild body size phenotype. *adt-2* RNAi treated worms have more severe body size defects. In addition to small body size RNAi treated worms show lethality. Deletion allele *tm975* is a null mutant which results in embryonic lethality. Trans heterozygote of *wk156/ tm975* enhanced mild body size phenotype in *wk156*. These observations clearly demonstrate that ADT-2 plays an important role in body size and development in *C. elegans*.

ADT-2 role in body size regulation might be conserved in mammals. Some examples are: *ADAMTS2* is associated with connective tissue disorders such as EDS (Ehlers-Danlos syndrome) in humans and with dermatosparaxis in cattle. Both disorders are characterized by fragility of skin and short body size (Colige et al. 1999; Lenaers et al. 1971). A mutation in *ADAMTS10* is associated with Weill-Marchesani syndrome (WMS), a disorder that is characterized by short body size, short fingers and toes, joint stiffness and eye anomalies (Dagoneau et al. 2004). A mutation in *ADAMTSL2* (ADAMTS-like2) leads to geleophysic dysplasia, a condition characterized by short body size and digit abnormalities (Le Goff et al. 2008). Sequence

variations associated with human height lie at or nearby *ADAMTS10*, *ADAMTS17* and *ADAMTSL3* (ADAMTS-like3) (Gudbjartsson et al. 2008; Lettre et al. 2008; Weedon et al. 2008).

Chapter 2: Genetic interactions of *adt-2* and other body size mutants in *C. elegans*

INTRODUCTION

Many mutations in *C. elegans* result in small body size indicating that the body size in *C. elegans* is in part genetically controlled. At least three different pathways determine the body size of *C. elegans*: *dbl-1* pathway (*dbl-1, sma-2, sma-3, sma-4, sma-9, kin-29 and lon-1*)(Patterson and Padgett 2000; Savage-Dunn, 2001; Savage-Dunn et al. 2003; Liang et al., 2003); spectrin pathway (*sma-1, spc-1* and *unc-70*)(Mckeon et al., 1998), sensory pathway (*egl-4, che-3, cnb-1* and *tax-6*)(Kuhara et al., 2002; Bandyopadhyay et al., 2002). Some of the small body size mutants have not yet been placed in these pathways. These include *rnt-1*, a homlogoue of mammalian RUNX transcription factor (Ji et al, 2005) and *sma-5,* a homolog of MAP kinase BMK1/ERK5 (Watanable et al., 2005).

When a new mutant is isolated, it is important to determine the interactions with other known mutants of the same phenotype. By doing this one can determine that the new component is acting in an existing pathway or in a novel pathway for its function. If two separate mutations result in reduced body length by separate pathways, homozygous double mutant should be smaller than either single mutant alone indicating that two mutations have additive effects. If one mutation results in long body size by affecting one pathway while a second mutation causes small body size affecting another pathway the double mutant will show additive effect with intermediate body size (Fig 14). Double mutants of *adt-2* and known pathways for body size regulation will help to determine the epistasis relationship between *adt-2* and known body size determinants.

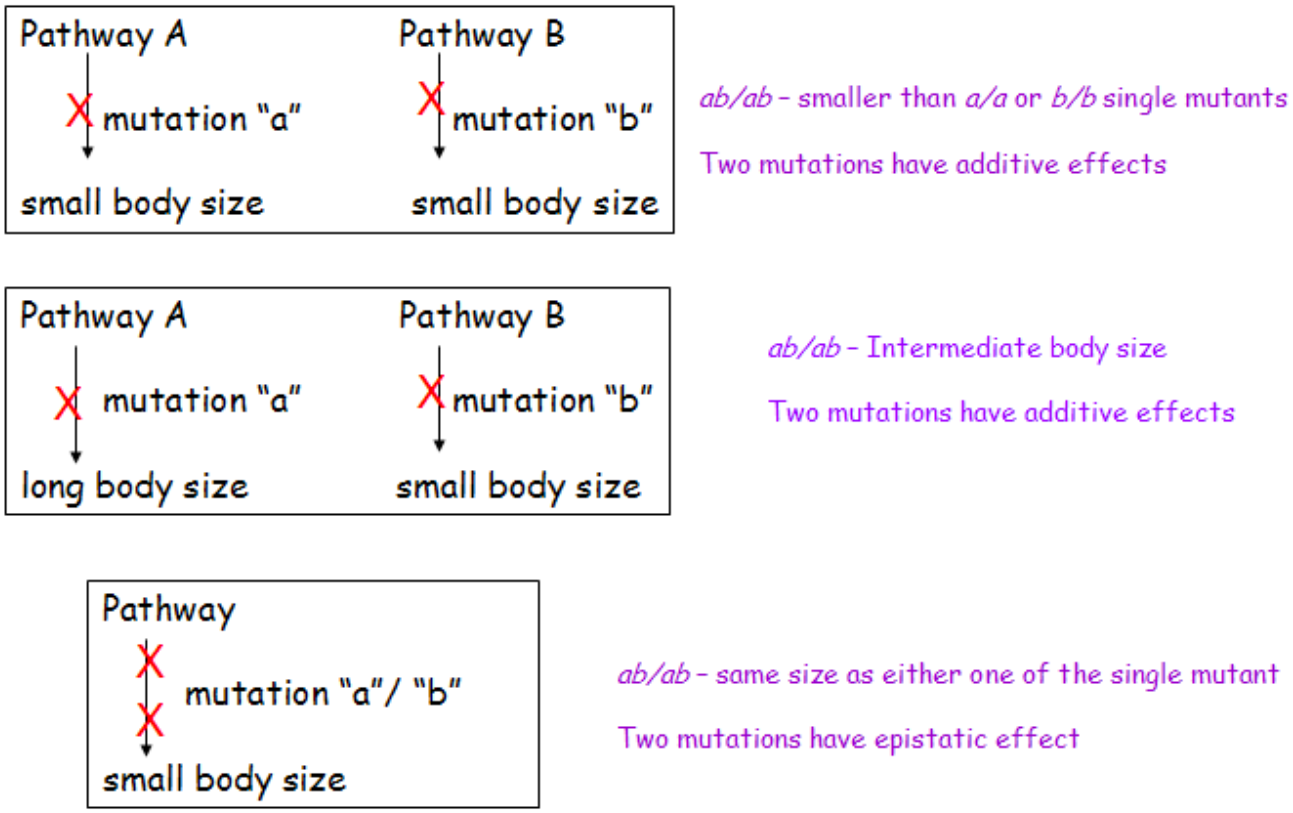

Figure 14. Genetic interaction between mutants

MATERIALS AND METHODS

Strains

C. elegans strains were grown at 20^0C using standard methods (Brenner, 1974), except for *daf-4*, which was grown at 15^0C to prevent constitutive dauer formation. In addition to strains generated in this study the following strains were used:

N2 and HA (wild type)

LG I: *rnt-1(ok351*)

LG II: *cnb-1(ok276)*

LG III: *sma-2(e502), sma-3(wk30), sma-4(e729)*, *daf-4(e1364)*

LG IV: *tax-6(ok2065)*, *egl-4(n477)*

LG V: *dbl-1(wk70), sma-1(e30)*, *him-5(e1490)*

LG X: *sma-9(wk55), che-2(e1033),*

Transgenics: *dbl-1(ctIs40)* (Suzuki et al., 1999)

Generations of double mutants:

Double mutants containing mutations in the *sma-6, daf-4, sma-2, sma-3, sma-4, sma-9, sma-1* and *rnt-1* genes were created by crossing *adt-2(wk156);him-5(e1490)* males into the hermaphrodites of each mutant and scoring progeny for the expected phenotypes. The *rnt-1(ok351)* deletion mutation was confirmed by PCR. All the other mutations were confirmed by complementation tests. *che-2(e1033);adt-2(RNAi), egl-4(n477);adt-2(RNAi),*

tax-6(ok2065);adt-2(RNAi), and *cnb-1(ok276);adt-2(RNAi),* double knockdowns were made by feeding *che-2*, *egl-4, tax-6,* and *cnb-1* mutant worms with *adt-2* dsRNA expressing bacteria.

Analysis of body size measurements:

For body length measurements of the single and double mutants, 96 hrs old worms (144 hrs for *daf-4* and *daf-4;adt-2* double mutant grown at 15^0C) were photographed using QC Capture 2.73.0 and the length was measured using Image-Pro Express 5.1.0.12 software.

RESULTS AND DISCUSSION

Genetic interactions of *adt-2* and other body size mutants in *C. elegans*:

The DBL-1 pathway plays a major role in body size regulation in *C. elegans*. Mutations in any components of the pathway, *dbl-1* (ligand), *sma-6* (type I receptor), *daf-4* (type II receptor), *sma-2*, *sma-3*, *sma-4* (Smad transcription factors), *sma-9* (transcription co-factor) will result in smaller bodies than wild type (Estevez et al. 1993; Krishna et al. 1999; Liang et al. 2003; Savage-Dunn 2005; Savage-Dunn et al. 2003; Savage et al. 1996; Suzuki et al. 1999). It was interesting to see whether ADT-2 modulates DBL-1/TGFβ signaling for several reasons. First, the DBL-1/TGFβ pathway has been known to induce ECM formation (Arnott et al., 2006). Second, a Tolloid protein (Astacin family metalloprotease) is known to function by forming a complex with Dpp/TGFβ in *Drosophila* (Finelli et al., 1995). Also in *Xenopus* Tolloid protein cleaves Chordin/Bone Morphogenetic Protein (BMP) complex to generate a gradient of BMP for dorsal ventral patterning of the embryo (Lee et al., 2009). Third, type IV collagen has been shown interact with Dpp (Wang et al., 2008). Double mutants were created in order to determine the relationship between *adt-2* and *dbl-1* pathway components. *dbl-1* pathway mutants we used for this were null or strong alleles**.** Double mutants of *adt-2(wk156)* combined with *dbl-1(wk70), sma-6(wk7), daf-4(e1364), sma-2(e502), sma-3(wk30), sma-4(e729)* or *sma-9(wk55)* have a smaller body size than the respective single mutants (Fig. 15A), which leads us to conclude that *adt-2* may act independently from the DBL-1 pathway to regulate body size.

To further validate this result, we looked at the *dbl-1* overexpression phenotype in the *adt-2* mutant background. Overexpression of *dbl-1* results in a long (Lon) body phenotype. The

Lon phenotype of *dbl-1* overexpression is suppressed in *sma-2*, *sma-3*, *sma-4*, *sma-6* or *daf-4* mutant backgrounds placing the activity of these small (Sma) genes downstream of the DBL-1 ligand activity (Suzuki et al. 1999). We fed *dbl-1* overexpressing worms on *adt-2* RNAi plates. However, rather than the expected complete suppression of the Lon phenotype, if the *adt-2* gene activity were downstream, the body length was intermediate. This is evidence that *adt-2* acts independently of the DBL-1 pathway (Table 4).

To determine whether *adt-2* interacts with other pathways that regulate body size, we next tested mutants in sensory processing. The *tax-6* and *cnb-1* genes encode calcineurin A and B subunits. Both *cnb-1* and *tax-6* are expressed in sensory neurons. Mutations in these genes cause pleiotropic defects including small body size and defects in sensory neuronal behavior (Bandyopadhyay et al. 2002; Kuhara et al. 2002). *cnb-1* also has a transparent appearance because of the thinning of the cuticle (Bandyopadhyay et al. 2002). *che-2* and *che-3* mutants also have a small body size phenotype. They have impaired sensory cilia and therefore defects in sensory perception. EGL-4, cGMP-dependent protein kinase acts downstream of *che* genes to regulate body size by repressing the *dbl-1* pathway (Fujiwara et al. 2002). In order to see whether *adt-2* functions in the chemosensory pathways, the double knockdowns between *adt-2* and *tax-6, cnb-1*, *che-2* and *egl-4* were made by combining existing chromosomal mutations and RNAi inactivation of *adt-2*. The *egl-4(n477);adt-2(RNAi)* double knockdowns have an intermediate body size compared to *egl-4* and *adt-2* single mutant animals. The *tax-6(ok2065);adt-2(RNAi), cnb-1(p675);adt-2(RNAi)* and *che-2(e1033);adt-2(RNAi)* double knockdowns also showed additive effects (Fig. 15B).

To test whether *adt-2* functions in the same pathways as *rnt-1* and *sma-1, rnt-1(ok351);adt-2(wk156)* and *sma-1(e30);adt-2(wk156)* double mutants were constructed. The

rnt-1 gene is the *C. elegans* homologue of mammalian RUNX transcription factors (JI et al. 2004). *sma-1* encodes for βH-spectrin (Mckeown et al. 1998)**.** Mutations in these genes cause small body size phenotype. Double mutants of *rnt-1(ok351);adt-2(wk156)* and *sma-1(e30);adt-2(wk156)* show additive effects (Fig. 15C). In all of these analyses, all of the double mutants showed additive effects and none of them demonstrate clear epistasis. Our data suggest two possibilities. One possibility is that ADT-2 acts parallel to these known pathways to regulate body size. The other possibility is that it is involved in multiple pathways to regulate the body size.

Figure 15. Genetic interactions of *adt-2* and other small body size mutants in *C. elegans*. In each graph first two bars represents N2 and *adt-2(wk156).* Subsequent bars represent the indicated single mutant and corresponding double mutant with *adt-2(wk156)*. Data are shown as a percentage of wild type body length. Each bar represents a mean of more than 27 adult animals measured at 96 hrs after embryo collection (except *daf-4* and *daf-4;adt*-2 which were grown at 15^0C for 144 hrs) . Error bars indicate the standard deviation. ** indicates $p<0.01$(t-test).

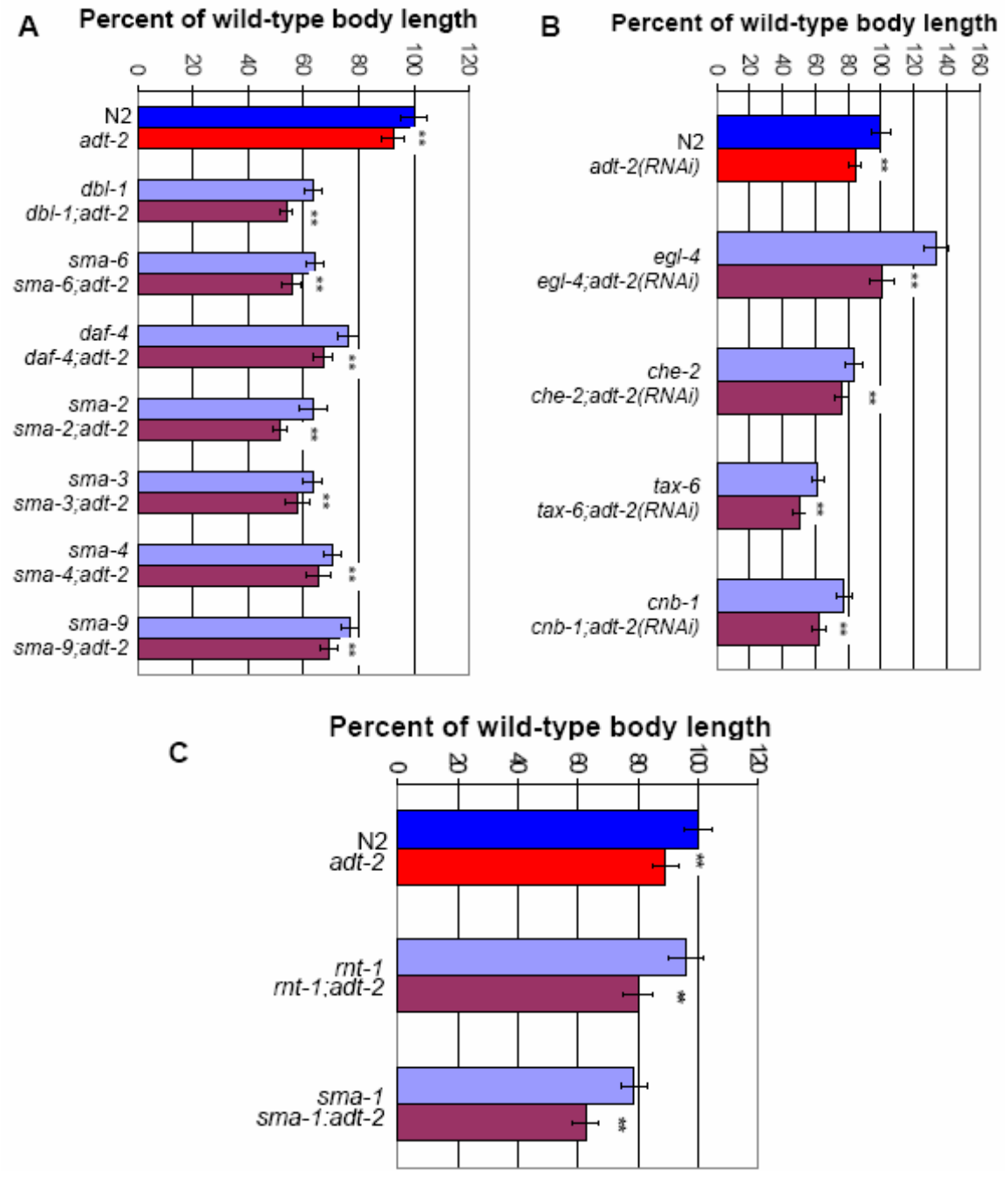
A
Percent of wild-type body length
0
20
40
60
80
100
120
N2
adt-2
dbl-1
dbl-1;adt-2
sma-6
sma-6;adt-2
daf-4
daf-4;adt-2
sma-2
sma-2;adt-2
sma-3
sma-3;adt-2
sma-4
sma-4;adt-2
sma-9
sma-9;adt-2
**
B
Percent of wild-type body length
0
20
40
60
80
100
120
140
160
N2
adt-2(RNAi)
egl-4
egl-4;adt-2(RNAi)
che-2
che-2;adt-2(RNAi)
tax-6
tax-6;adt-2(RNAi)
cnb-1
cnb-1;adt-2(RNAi)
**
C
Percent of wild-type body length
0
20
40
60
80
100
120
N2
adt-2
rnt-1
rnt-1;adt-2
sma-1
sma-1;adt-2
**
*

TABLE 4. *adt-2* did not fully suppress the Lon phenotype of *dbl-1* overexpression

Genotype	Body length in adult animals	n
N2	1.193 +/- 0.065	33
adt-2	1.004 +/- 0.048	28
ctIs40[pTG96(sur-5::gfp); dbl-1(++)]	1.336 +/- 0.069	33
adt-2; ctIs40[pTG96(sur-5::gfp ;dbl-1(++)] [1, 2]	1.177 +/- 0.07	33

[1] Value is not significantly different from N2, $p>0.05$
[2] Values are significantly different from *adt-2* and *ctIs40*, $p<0.0001$(t-test)

Chapter 3. ADT-2 functions in the cuticle by modifying cuticle collagen organization.

INTRODUCTION

The entire body of the *C. elegans* is covered by a collagenous cuticle that is known to play a major role in controlling the body size of the animal. Animals with mutations in the genes that encode collagen have body size defects. Some examples of these mutations are *dpy-2*, *dpy-7*, *dpy-10, dpy-13*, *sqt-1*, *sqt-3* and *lon-3*. (Johnstone et al., 1992; Kramer, 1994; Kramer and Johnson, 1993; Kramer et al., 1988; Levy et al., 1993; Nystrom et al., 2002; Suzuki et al., 2002; van der Keyl et al., 1994; von Mende et al., 1988). The question is does ADT-2 act in the cuticle to regulate the body size similar to the collagen mutants?

Collagens in the cuticle are synthesized as procollagens with N- and C- terminus pro-collagen domains. These pro domains must be processed in order to syntheze a mature collagen molecule that can be organized into higher ordered structures (Van der Rest et al., 1991; Hulmes, 1992; Prockop at al., 1995; Wang et al., 2006). There are three groups of identified substrates for mammalian ADAMTS. First, procollagen: processed by ADAMTS-2, -3 and -14; second, proteoglycans: processed by ADMTS-1, -4, -5, -8, -9 and -15; third, von Willebrand factor: processed by ADAMTS-13 (Colige et al., 1995; Colige et al., 1997; Collins-Racie et al., 2004; Fernandes et al., 2001; Kuno et al., 2000; Somerville et al., 2003; Tortorella et al., 2000; Tortorella et al., 2005; Wang et al., 2003; Jones et al, 2005).

ADT-1 in *C. elegans* is required for the morphogenesis of male copulatory organs, a process that requires rapid remodeling of the cuticle (Kuno et al., 2002). Sequence similarity data in the chapter 1 also show that the catalytic domain of the ADT-2 has high similarity to the catalytic domain of the mammalian procollagenase and ADT-1 in *C. elegans*. This information suggests that ADT-2 might also act as a collagenase that is required for ECM assembly. In order to see whether this hypothesis is correct, the cuticle of the *adt-2* mutants was examined

first. Examined second was the expression pattern of the transcriptional and translational adt-2::GFP reporter. Lastly, a western blot was performed to see whether ADT-2 processes COL-19.

MATERIALS AND METHODS

adt-2(p)::GFP expression:

We used PCR fusion based approach to create *sma-21(p)::GFP* construct (Hobert 2002). We amplified 4492bp region of genomic DNA upstream of *adt-2* to the nearest adjacent gene and fused with a GFP reporter. Primers used for fusion were:

adt-2A: 5' GC GGA TCC TAA AAC TAT AGG AAA TTC GGA 3

adt-2A*: 5' GC GGA TCC TTT ATG TAA TAC TAA TAC TGG 3'

adt-2B: 5' GAA AAG TTC TTC TCC TTT ACT CAT aat gtt gtt ctg gag ttg gca gaa 3'

adt-2B*: 5' GAA AAG TTC TTC TCC TTT AC TCA Ttg aga ata tgc aga ttt cac aac g 3'

20 ng/µl *adt-2(p)::GFP* construct was microinjected to N2 hermaphrodites along with myo-3::mcherry as a transformation marker. Total concentration of the DNA at injection was adjusted to 100 ng/µl using Bluescript SK.

COL-19::GFP localization in *adt-2(wk156)*:

In order to see the cuticle of *adt-2(wk156),* an adult specific marker COL-19::GFP was used (Thein et al. 2003). kaIs[*col-19::gfp*];*adt-2(wk156)* was constructed by crossing COL-19::GFP males into *adt-2(wk156)* hermaphrodites. The small hermaphrodites with COL-19::GFP were picked in the F2 generation. Plates bearing smalls and COL-19::GFP were selected and the cuticle was observed under the confocal microscope. kaIs[*col-19::gfp*];*adt-2(tm975/wk156)* was made by crossing kaIs[*col-19::gfp*];*adt-2(wk156)* males into *adt-2(tm975)/+* hermaphrodites. We also treated COL-19::GFP worms on *adt-2(RNAi).*

ADT-2::GFP translational construct

We used fosmid based reporter gene construct to generate a ADT-2::GFP translational construct (Tursun et al. 2009). A cassette containing GFP was inserted by homologous recombination at the C- terminus of *adt-2* in a fosmid containing *adt-2*. A cassette containing GFP and a selectable marker galactose kinase (galK) (GFPint - *FgF*) was kindly provided by Dr. Oliver Hobert's lab. Homology arms were added to the cassette containing GFP using following primers.

GFPint-fgf -F

5' cgaaaagcaatactgtaatttgcgtgtttgcgacttccgaagaaagtttatgagtaaaggagaagaacttttcac

GFPint-fgf –R

5' tattcgatcagacttttggaaaagatcgtataatttgtttccctttcgattttatttgtatagttcatccatgccatg

At the 5' end of each primer there is about 50 bp sequence homologous to each side of the site of the insertion. First, E *coli* strain SW105 (galK defective, contains HS inducible λ red recombinase and Ara inducible Flp recombinase) was transformed with the fosmid containing *adt-2* by electroporation. Single colonies were grown and heat shocked at 42 C^0 for 20 minutes. Next, the cassette containing GFP with homology arms was introduced by elecroporation into the SW105 strain, which has the fosmid in it. At this stage, homologous recombination took place and the colonies were selected on the minimal medium with galactose. These colonies were streaked on MacConkey agar plates to confirm the galactose kinase activity. Colonies with galk activity change the pH of the medium and turn red. Finally, these colonies were grown and treated with Arabinose to induce flippase to get rid of the selectable marker gene. Correct

insertion and the excision of the *FgF* module were confirmed by the following flanking PCR primers.

Adt-2 F11 – 5' aat cac tga cca atc gtc gtc 3'

Adt-2 R11 – 5' gca aat gag caa cga caa atg

Original fosmid was used as a control (Fig. 18A). Flanking primers produce about 2845bp fragment when the original fosmid was used as the template. Insertion of GFP causes a size increase of about 2000bp which resulted in 5045. Excision of the selectable marker a decrease by about 1300 bp which resulted in 4345bp (Fig. 18 A). Fosmids which give the correct band patterns were electroporated back to the strain EPI300 for maintenance. 10 ng/µl ADT-2::GFP construct was microinjected to *adt-2* hermaphrodites along with *myo-3*::mcherry as a transformation marker. Total concentration of the DNA at injection was adjusted to 100 ng/µl using Bluescript SK. Mixtures of fosmids were used with digested worm genomic DNA for formation of complex arrays as described in Tursun *et al*. 2009. 10 ng/µl of fosmid DNA together with worm genomic DNA at 150 ng/µl and the myo-3:: mcherry marker at 5ng//µl (digested with SmaI) were microinjected to the *adt-2* worms.

Western blot

Worms were washed off with M9 buffer, spun down and boiled for 5 minutes in sample buffer. After spinning for 10 minutes at 10000 rpm, the supernatant was transferred into a new tube. 30 µl of the protein samples were loaded in to the gel and SDS-PAGE was carried out on a mini-protein electrophoresis apparatus. Proteins in SDS-polyacrylamide gels were transferred to nitrocellulose membrane at 100V for 1 hr. After transfer, the nitrocellulose membrane was immersed in Blocking buffer (5% dry-milk in PBST) and blocked overnight at 4 C^0. Then, the

membrane was washed with PBST and incubated with the primary antibody anti-GFP (Rabbit Anti-GFP Clontech). Again the membrane was washed with PBST to remove excess or unbound antibodies and incubated with the secondary antibody anti-rabbit IgG. Once more the membrane was washed to get rid of unbound secondary antibodies. ECF detection was performed according to the manufacturer's instructions (Amersham).

Immunostaining

Immunostaining was performed as described in CSHL worm Course 2006 (cshprotocols.cshlp.org/cgi/content/full/2006/23/pdb.prot4522). Fixed worms were stained with primary antibody anti-GFP (Rabbit Anti-GFP Clontech). The secondary antibody was anti-rabbit IgG. Fluorescence was observed using Nikon inverted microscope.

Results and Discussion

adt-2 may regulate body size in part by modification of the external cuticle

To test whether ADT-2 acts to regulate cuticle collagen organization, we used a COL-19::GFP protein fusion (Thein et al., 2003) to visualize the cuticle collagen fibrils in *adt-2* mutant and RNAi animals. This reporter construct is expressed in annuli and lateral alae of the adult cuticle (Thein et al., 2003; Fig. 16A). As shown in Figure 16C, animals treated with *adt-2(RNAi)* showed significant disruptions of the lateral cuticle overlying the seam cells. We also detected constrictions of the annuli in *adt-2(RNAi)* worms (Fig. 16B and Table 5). We analyzed COL-19::GFP expression in *adt-2(wk156)* and in *adt-2(tm975/wk156)* transheterozygous animals using fluorescence and normaski microscope. The localization was not significantly altered in *adt-2(wk156)* mutants, however, the annuli were constricted (Table 5). Thein et al, 2003 have suggested that the short distance between annuli could be due to excessive lateral constriction. In *adt-2* mutants, lateral constriction could result in a shorter body length. Alternately, it could be a secondary defect caused by disrupted cuticle over the seam cells. Analysis of COL-19::GFP expression in *adt-2(tm975/wk156)* revealed patches of disorganized annuli (Fig. 16C). Defects in the alae were observed in *adt-2(wk156)* and *adt-2(wk156/tm975)*. The defects are discontinuous alae and alae with two or four ridges as compared to three ridges in the wild-type worms (Fig. 16 D, E, F, G). These defects are similar to the cuticle defects seen in the collagen mutants such as *dpy-5, dpy-13*, and *bli-1*, and in *col-19(RNAi)* animals. Interestingly, *adt-2* was also previously identified in an RNAi screen for genes required for molting of the cuticle (Craig et al. 2007; Frand et al. 2005). These data show that ADT-2 acts in the cuticle and is required for normal cuticle structure. Disruption in cuticle

structure or the collagen organization may explain the reduced body size in *adt-2* mutants and knockdowns.

Figure 16: Aberrant COL-19::GFP localization in *adt-2* mutants. (A,B,C) COL-19::GFP expression. In wild-type animals, COL-19::GFP fusion protein is expressed in annuli extending over most of the dorsal and ventral cuticle (A). RNAi inactivation of *adt-2* causes an expanded region of disruption in the lateral cuticle (double headed arrow; B). Patches of the disorganization of the annuli are also evident in the *adt-2(tm975/wk156)* adult worms (C). (D,E,F and G) Nomarski microscopy image of cuticular alae. The cuticle of adult wild-type hermaphrodite shows lateral alae with three characteristic ridges (D). Nomarski microscopy images of the cuticle of *adt-2(wk156)* showing abnormal number (arrowheads) and discontinuation (asterisks) of the alae (E). *adt-2(tm975/wk156)* hermaphrodites show abnormal numbers of alae (arrowheads; four in G and two in F), as well as discontinuous alae (asterisk; G).

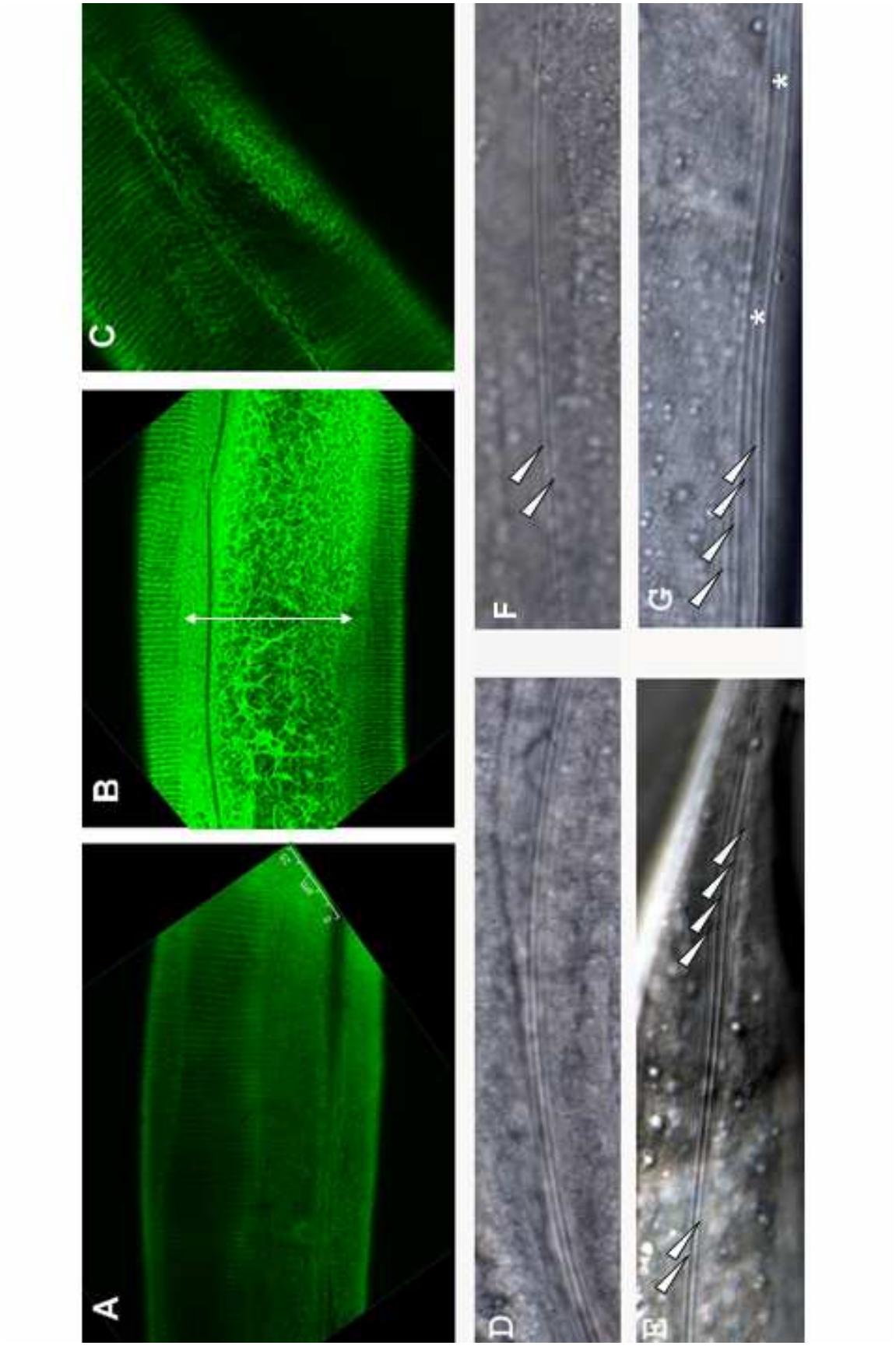
A
B
C
D
E
F
G
*
*

Table 5. *adt-2(RNAi)* and *adt-2(wk156)* worms have constricted annuli

Genotype	Distance between annuli (μm)	Number of annuli	Number of worms
TP12: *kaIs12*[COL-19::GFP]	1.809 +/- 0.18	390	15
kaIs12[COL-19::GFP];*adt-2(wk156)*	1.478 +/- 0.14**	688	20
TP12: *kaIs12*[COL-19::GFP] (RNAi control)	1.656 +/- 0.20	459	17
kaIs12[COL-19::GFP]; *adt-2(RNAi)*	1.437 +/- 0.16**	690	21

**$p<0.01$

***adt-2(p):: GFP* expression.**

To determine the expression pattern of *adt-2,* we followed the expression of a transcriptional fusion of GFP to putative *adt-2* promoter sequences. No expression was seen in embryonic stages. GFP expression was detected in glial cells associated with amphid, phasmid, labial and posterior deirids (PDE) sensory neurons as early as the L1 stage and continued throughout larval development (Fig. 17). Expression was also seen in vulval tissue in L4 and adult animals. We note that these glial and vulval cells are in close association with the external cuticle, (Fig. 17E) so it is possible that ADT-2 exerts its influences by proteolytic processing of cuticle proteins such as collagen. C- terminal thrombospondin repeats may be playing a role in ECM binding as in ADAMTS in mammals (Kuno et al., 1998). It has been shown that Zn metalloprotease NAS-37 belongs to family astacin is synthesized in glia – like cells and secreted to the cuticle (Davis et al. 2004). Glia- like cells in *C. elegans* have also found to be enriched in expression of extracellular proteins including some metalloproteases (Bacaj, et al., 2008).

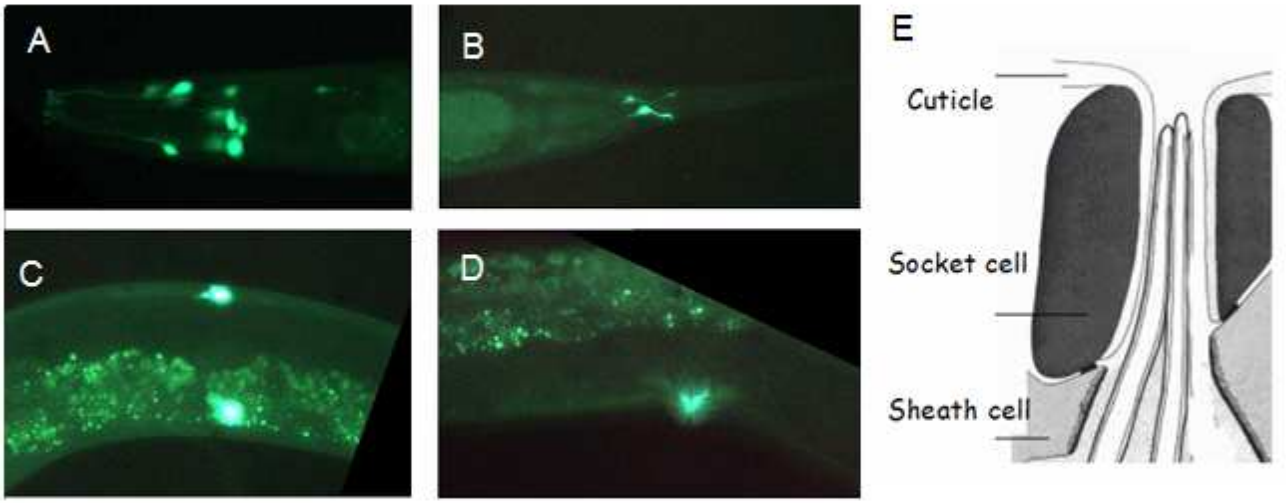

Figure 17. Expression patterns of ***adt-2p::gfp***. *adt-2* is expressed in the glial cells of (A) amphid and labial neurons (B) phasmids (C) postdeirid and (D) in the vulva. E) Diagrammatic view showing socket cells associated with cuticle (Wormbook).

ADT-2::GFP localization:

To elucidate the function of ADT-2 in body size regulation, I examined its expression pattern. Mixtures of recombineered fosmids containing GFP reporter gene at the C terminus of *adt-2* was injected into *adt-2(wk156)* animals. A total of nine independent lines were obtained. Six of the rescued the small body size phenotype of the *adt-2(wk156)*(Fig. 18B and C). This shows that incorporation of GFP has not affected the function of the ADT-2 in body size regulation. From the worms that rescued the small body size phenotype, in about 10% of the adult worms, ADT-2::GFP is localized into the lateral alae of the cuticle (Fig. 18D). However, the alae defects in the number of the ridges are not completely rescued as two or four ridges were still observed instead of three in the wild type worms. ADT-2::GFP expression also can be seen in vulva (Fig. 18E). In order to see whether there is any increase of the GFP signal and/or to find out whether ADT-2::GFP is localized into any other places, rescued worms were immunostained for GFP using anti-GFP antibodies. Immunostained worms showed ADT-2 localization in the annuli and the alae of the cuticle (Fig. 18 F and G). Immunostaining has increased the frequency and the signal strength to a much higher level than non-immunostained worms. The localization of ADT-2 in the alae shows that the defects seen in the alae of *adt-2* mutants must be due to loss of function of ADT-2. Also the localization of ADT-2 in the alae of the cuticle supports the hypothesis that ADT-2 can act as a procollagen N- proteinase.

Figure 18. ADT-2::GFP localization. A) Analysis of PCR product from recombineered fosmid. Lane 1 is the original fosmid which gives about 2845bp fragment. Insertion of the GFP cassette increases the size of the PCR product to 5045 in lane 3,5,7 and 8. Lanes 2, 4, 6 and 9 are after the excitation of the *FgF* module. Size is decreased to about 4345bp (A). ADT-2::GFP reporter construct rescues the small body size in *adt-2(wk156)* mutant (B and C). ADT-2::GFP is localized to the lateral alae (D,G arrow) annuli (F, arrows) and in the vulva (E).

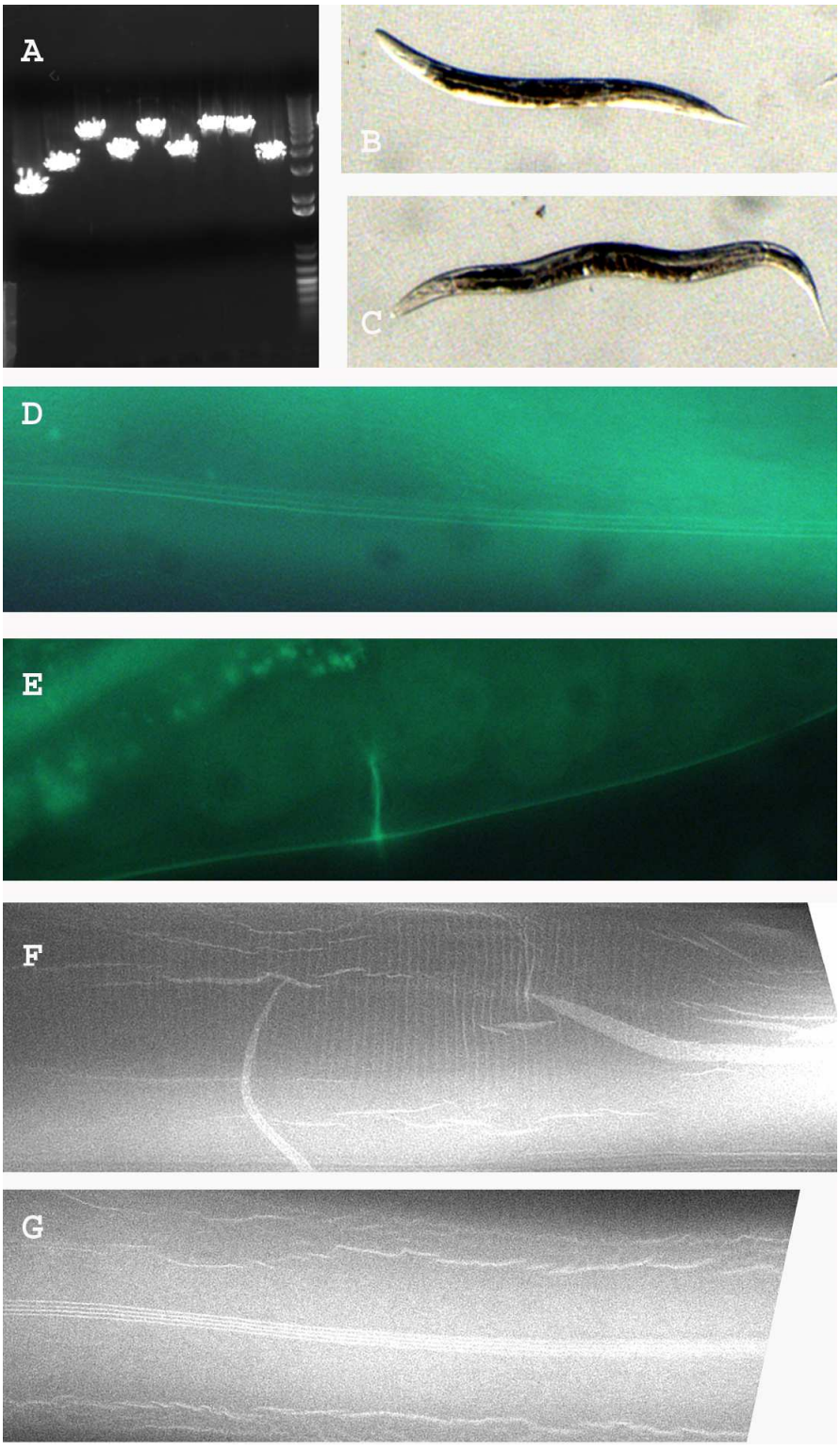
A
B
C
D
E
F
G

Does ADT-2 process COL-19?

To test the hypothesis that ADT-2 processes collagen, I assayed changes in protein processing of COL-19::GFP by western blot analysis. Total protein was isolated from adult and young adults of wildtype COL-19::GFP, COL-19::GFP; *adt-2(wk156)* and COL-19::GFP; *adt-2*(RNAi) worms. Proteins in SDS-polyacrylamide gels were transferred to nitrocellulose membrane, incubated with the primary antibody anti-GFP (Rabbit Anti-GFP Clontech) and the secondary antibody anti-rabbit IgG. The protein mobility pattern was analyzed. Unprocessed COL-19::GFP fusion protein is about 58KD. Removal of predicted prodomain of COL-19 should give about 52KD product which should migrate at faster rate. Low mobility bands at the top of the gel are due to the formation of higher ordered multimers with other or the same collagen fibrils via non-reducing di- and tri- tryrosine cross-links (Fujimoto et al., 1981; Fetterer, et al., 1993 and Yang et al., 1999). Results of the western blot do not show clear evidence of ADT-2 processing COL-19 as we cannot see any difference in the amount of processed COL-19::GFP (Fig. 19).

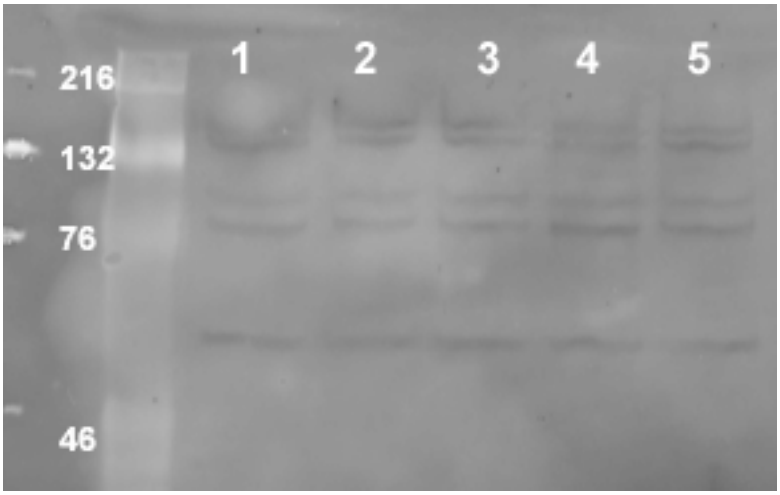

Fig. 11. Western blot analyses of TP12 wild type and *adt-2* mutant worm protein extract with anti-rabbit GFP antibodies. TP12: *kaIs12*[COL-19::GFP](L1, L4), *kaIs12*[COL-19::GFP];*adt-2(wk156)*(L2, L4) and *kaIs12*[COL-19::GFP]; *adt-2(RNAi)* (L5). The molecular weight standards are indicated in kilo Daltons to the left.

Conclusion

In this study a novel determinant of body size, ADT-2, was characterized. ADT-2 belongs to the ADAMTS family, which is known to play a major role in ECM (extracellular matrix) assembly and degradation. Animals that lack ADT-2 activity show body size defects, indicating ADT-2 is involved in body size regulation. Once ADT-2 was identified, the question that remained was how exactly does ADT-2 regulate body size? It was found that ADT-2 does not interact with other known determinants to regulate the body size. I hypothesized that ADT-2 acts in the cuticle as a pro-collagen protease, which is vital to the structure of the cuticle. This hypothesis is based on the following pieces of evidence. (1) Collagen organization defects seen in the cuticle of *adt-2* mutants clearly show that ADT-2 exerts its effect in the cuticle to regulate the body size. (2) Upon examination of the expression pattern, ADT-2::GFP was observed to be localized in the cuticle. It is interesting to see that *adt-2(p)::gfp* is expressed in only specific types of cells but ADT-2::GFP is localized throughout the cuticle. The difference might be due to the fact that *adt-2(p)::gfp* has only upstream sequences and so may be missing other important regulatory sequences. Also, it is possible that the GFP signal level was so low or diffused in the hypodermis that the signal was undetectable. (3) The metalloprotease domain of ADT-2 shows the highest similarity to mammalian Procollagen N-proteinases ADAMTS-2, -3, and -14.

There is however, one negative result that contradicts the hypothesis: we saw no evidence for ADT-2 processing COL-19::GFP *in vivo*. Even though we did not see ADT-2 process COL-19::GFP, it is possible that ADT-2 might be processing collagens other than COL-19. It may be that ADT-2 shows substrate specificity for particular group of collagen other than group I (grouping is based on the position of conserved cysteines in Gly-X-Y interruptions). In

group 1 the number of amino acid residues between conserved cysteines in domain I and II is 41-42 and in domain II and III is about 133 (Johnstone, 2000).

In *C. elegans* one ECM, the cuticle, plays a major role in determining body size due to the fact that it encapsulates *C. elegans*. *adt-2* mutants show a series of defects in the cuticle including extended disruption in the lateral cuticle, discontinuities and an abnormal number of ridges in the alae. These defects are reminiscent of defects reported in a subset of cuticle collagen mutants such as *dpy-5, dpy-13*, and *bli-1*, and in *col-19(RNAi)*. Due to the defects in the cuticle of *adt-2* mutants, the cuticle may not be able to maintain its integrity, which leads to the resultant defect in body size. These defects in the cuticle can also explain the reason for early death of *adt-2* mutants by an increased vulnerability to injuries and infection. Also *adt-2(wk156)* mutants shrink as they grow from 96 hrs to 120 hrs after embryo collection. Loss of cuticle integrity might cause the worm to be more compressed inside the cuticle. Since ECM is known to influence the activity of signaling pathways, our results do not exclude the possibility that ADT-2 also regulates body size in part by indirect modulation of DBL-1 or other growth factor signals. The finding of ADT-2 localization in the lateral cuticle (alae) indicates nonautonomous effect on reduced seam cell size in *adt-2* mutants.

A model for ADT-2 regulation of body size: Based on the phenotype, expression pattern, and cuticle defects associated with *adt-2*, we describe the following model for its regulation of body size. ADT-2 is expressed in support cells of sensory neurons, and secreted into the external cuticle. By associating with the ECM of the cuticle, ADT-2 may be in contact

with secreted procollagen trimers. Based on the homology of ADT-2 with procollagen N-proteinases, we propose that ADT-2 participates in the processing of procollagens by cleaving their N-terminal prodomains which is important for the normal organization of the target fibrils and/or their cross-linking to form higher ordered structures. Upon the reduction of ADT-2 activity, defects in collagen fibril organization are apparent and are associated with the degree of reduction in body size.

Many of the proteins in organisms are synthesized as precursor proteins. They have to undergo proteolytic processing in order to perform their function in the organism. Collagen is one of the proteins which belong to this group. Collagen is present in the majority of the tissues and organs including the skin, tendon, bones and basement membranes. ADAMTS has a major role in cleaving the ends of the collagen to become mature allowing it to function properly. Production of new collagen and their proper processing must be necessary for the proper deposition of collagen in these tissues, which otherwise can cause abnormalities. Mutations in ADAMTS proteins lead to a variety of connective diseases and disorders such as Ehlers-Danlos syndrome and Weill-Marchesani syndrome in humans.

It has been found out that TS repeats and the spacer region in ADAMTS are important in ECM binding (Kuno and Matsushima 1998). If subcloning of the *adt-2* genomic region is a possibility, protease independent activity of ADT-2 such as substrate specificity, binding to the ECM and the role of different domains in this function can be assessed via structure functional analysis. Available transformation techniques will make *C. elegans* a great model system to perform these tests. Body size defects seen in *adt-2* mutants can be suppressed by affecting other independent

pathways as *adt-2;egl-4*, *adt-2; ctIs40[pTG96(sur-5::gfp) ;dbl-1(++)]* doubles show suppression of small body size in *adt-2*. So it may not be necessary to fix the individual mutation but rather simply bypass its function to correct defects. This can be applied to other organisms too. Defects in the growth associated with inherited syndromes such as EDS in humans and cattle and WMS in humans may be cured or at least reduced in severity by affecting similar pathways. Furthermore, genetic screens for suppressor mutations of *adt-2* will also provide valuable information for diseases associated with ADAMTS in humans and other organisms.

Therefore these findings already provide insights for the role of ADAMTS proteins in connective tissue physiology and body size regulation in other organisms.

References

ARNER E.C. 2002 Aggrecanase-mediated cartilage degradation. Curr Opin Pharmacol **2:** 322-329

ARNOTT J. A., E. NUGLOZEH , M.C. RICO, I. ARANGO-HISIJARA, P.R. ODGREN, F.F. SAFADI, S.N. POPOFF, 2006 Connective tissue growth factor (CTGF/CCN2) is a downstream mediator for TGF-β1-induced extracellular matrix production in osteoblasts**.** Journal of Cellular Physiology. **210:** 843 – 852

BACAJ T., M. TEVLIN, Y. LU, S. SHAHAM 2008 Glia Are Essential for Sensory Organ Function in C-elegans. Science **322**:744-747

BANDYOPADHYAY, J., J. LEE, J. LEE, J. I. LEE, J. R. YU *et al.*, 2002 Calcineurin, a calcium/calmodulin-dependent protein phosphatase, is involved in movement, fertility, egg laying, and growth in Caenorhabditis elegans. Mol Biol Cell **13:** 3281-3293.

BLELLOCH, R., and J. KIMBLE, 1999 Control of organ shape by a secreted metalloprotease in the nematode Caenorhabditis elegans. Nature **399:** 586-590.

BOHNI, R., J. RIESGO-ESCOVAR, S. OLDHAM, W. BROGIOLO, H. STOCKER *et al.*, 1999 Autonomous control of cell and organ size by CHICO, a Drosophila homolog of vertebrate IRS1-4. Cell **97:** 865-875.

BORNSTEIN P. 1992 Thrombospondins: structure and regulation of expression FASEB J. **6:**3290–3299.

BRASS L., 2001 VWF meets the ADAMTS family. Nature Medicine **7:**1177 - 1178

BRENNER, S., 1974 The genetics of Caenorhabditis elegans. Genetics **77:** 71-94.

RUSSELL R.L., AND R.C. CASSADA 1975. The dauerlarva, a post-embryonic developmental variant of the nematode C. elegans. Developmental Biology **46:**326-342

CHEN, C., J. JACK and R. S. GAROFALO, 1996 The Drosophila insulin receptor is required for normal growth. Endocrinology **137:** 846-856.

CHEN, L., T. MCCLOSKEY, P. M. JOSHI and J. H. ROTHMAN, 2008 *ced-4* and proto-oncogene *tfg-1* antagonistically regulate cell size and apoptosis in *C. elegans*. Curr Biol.**2**:1025-33

COLIGE, A., A. BESCHIN, B. SAMYN, Y. GOEBELS, J. VAN BEEUMEN *et al.*, 1995 Characterization and partial amino acid sequencing of a 107-kDa procollagen I N-proteinase purified by affinity chromatography on immobilized type XIV collagen. J Biol Chem **270:** 16724-16730.

COLIGE, A., S. W. LI, A. L. SIERON, B. V. NUSGENS, D. J. PROCKOP *et al.*, 1997 cDNA cloning and expression of bovine procollagen I N-proteinase: a new member of the superfamily of zinc-metalloproteinases with binding sites for cells and other matrix components. Proc Natl Acad Sci. **94:** 2374-2379.

COLIGE, A., A. L. SIERON, S. W. LI, U. SCHWARZE, E. PETTY *et al.*, 1999 Human Ehlers-Danlos syndrome type VII C and bovine dermatosparaxis are caused by mutations in the procollagen I N-proteinase gene. Am J Hum Genet **65:** 308-317.

COLLINS-RACIE, L. A., C. R. FLANNERY, W. ZENG, C. CORCORAN, B. ANNIS-FREEMAN *et al.*, 2004 ADAMTS-8 exhibits aggrecanase activity and is expressed in human articular cartilage. Matrix Biol **23:** 219-230.

CRAIG, H., R. E. ISAAC and D. R. BROOKS, 2007 Unravelling the moulting degradome: new opportunities for chemotherapy? Trends Parasitol **23:** 248-253.

DAGONEAU, N., C. BENOIST-LASSELIN, C. HUBER, L. FAIVRE, A. MEGARBANE *et al.*, 2004 ADAMTS10 mutations in autosomal recessive Weill-Marchesani syndrome. Am J Hum Genet **75:** 801-806.

DAVIS, M. W., A. J. BIRNIE, A. C. CHAN, A. P. PAGE and E. M. JORGENSEN, 2004 A conserved metalloprotease mediates ecdysis in Caenorhabditis elegans. Development **131:** 6001-6008.

DAVIS, M. W., M. HAMMARLUND, T. HARRACH, P. HULLETT, S. OLSEN *et al.*, 2005 Rapid single nucleotide polymorphism mapping in C. elegans. BMC Genomics **6:** 118.

ESTEVEZ, M., L. ATTISANO, J. L. WRANA, P. S. ALBERT, J. MASSAGUE *et al.*, 1993 The daf-4 gene encodes a bone morphogenetic protein receptor controlling C. elegans dauer larva development. Nature **365:** 644-649.

FERNANDES, R. J., S. HIROHATA, J. M. ENGLE, A. COLIGE, D. H. COHN *et al.*, 2001 Procollagen II amino propeptide processing by ADAMTS-3. Insights on dermatosparaxis. J Biol Chem **276:** 31502-31509

FETTERER, R. H., M. L. RHOADS, and J. F. URBAN JR., 1993. Synthesis of tyrosine-derived cross-links in *Ascaris suum* cuticular proteins. Journal of Parasitology **79:**160–166..

FINELLI A.L., T. XIE, C. A. BOSSIE, R. K. BLACKMAN, R. W. PADGETT (1995) The tolkin Gene Is a tolloid/BMP-1 Homologue That Is Essential for *Drosophila* Development. Genetics **141:**271-281

FLEMMING, A.J., Z. Z. SHEN, A. CUNHA, S. W. EMMONS and A. M. LEROI, 2000 Somatic polyploidization and cellular proliferation drive body size evolution in nematodes. *Proc Natl Acad Sci USA* **97:** 5285-90

FUJIMOTO, D., K. HORIUCHI and M. HIRAMA, 1981 a new crosslinking amino acid isolated from Ascaris cuticle collagen. Biochem Biophys Res Commun*Biochem. Biophys. Res.Commun.* **99:** 637–643

FRAND, A. R., S. RUSSEL and G. RUVKUN, 2005 Functional genomic analysis of C. elegans molting. PLoS Biol **3:** e312.

FUJIWARA, M., P. SENGUPTA and S. L. MCINTIRE, 2002 Regulation of body size and behavioral state of C. elegans by sensory perception and the EGL-4 cGMP-dependent protein kinase. Neuron **36:** 1091-1102.

GALLANT, P., Y. SHIIO, P. F. CHENG, S. M. PARKHURST and R. N. EISENMAN, 1996 Myc and Max homologs in Drosophila. Science **274:** 1523-1527.

GOLDEN, J.W., and D. L., RIDDLE, 1984b The *Caenorhabditis elegans* dauer larva: developmental effects of pheromone, food, and temperature. Dev. Biol. **102**, 368–378

GUDBJARTSSON, D. F., G. B. WALTERS, G. THORLEIFSSON, H. STEFANSSON, B. V. HALLDORSSON *et al.*, 2008 Many sequence variants affecting diversity of adult human height. Nat Genet **40:** 609-615.

GRAHAM R., 2005 Domain structure of matrix metalloproteinases (MMPs) and ADAMTS Expert Reviews in Molecular Medicine **7:** 1-25

HASHIMOTO, G., M. SHIMODA and Y. OKADA, 2004 ADAMTS4 (aggrecanase-1) interaction with the C-terminal domain of fibronectin inhibits proteolysis of aggrecan. J. Biol. Chem. **279**: 32483–32491

HESSELSON, D., C. NEWMAN, K.W. KIM and J. KIMBLE, 2004 GON-1 and fibulin have antagonistic roles in control of organ shape, *Curr. Biol* **14**: 2005-10

HOBERT, O., 2002 PCR fusion-based approach to create reporter gene constructs for expression analysis in transgenic C. elegans. Biotechniques **32:** 728-730.

HOLMBECK, K., P. BIANCO, J. CATERINA, S. YAMADA, M. KROMER *et al.*, 1999 MT1-MMP-deficient mice develop dwarfism, osteopenia, arthritis, and connective tissue disease due to inadequate collagen turnover. Cell **99:** 81-92.

HULMES D. J., 1992 The collagen superfamily – diverse structures and assemblies. *Essays Biochem.* **27**: 49–67

IHARA, S., and K. NISHIWAKI, 2007 Prodomain-dependent tissue targeting of an ADAMTS protease controls cell migration in Caenorhabditis elegans. Embo J **26:** 2607-2620.

INOUE, T., and J. H. THOMAS, 2000 Targets of TGF-β signaling in *Caenorhabditis elegans* dauer formation. Dev. Biol. **217**, 192–204

YANG J. and J. M. KRAMER, 1999 Proteolytic Processing of *Caenorhabditis elegans* SQT-1 Cuticle Collagen Is Inhibited in Right Roller Mutants whereas Cross-linking Is Inhibited in Left Roller Mutants. The Journal of Biological Chemistry **274:** 2744–32749

JARRIAULT, S. and I. GREENWALD, 2005 Evidence for Functional Redundancy Between *C. elegans* ADAM Proteins SUP-17/Kuzbanian and ADM-4/TACE. *Dev Biol*. **287**: 1–10.

JI, Y. J., S. NAM, Y. H. JIN, E. J. CHA, K. S. LEE *et al.*, 2004 RNT-1, the C. elegans homologue of mammalian RUNX transcription factors, regulates body size and male tail development. Dev Biol **274:** 402-412.

JOHNSTON, L. A., D. A. PROBER, B. A. EDGAR, R. N. EISENMAN and P. GALLANT, 1999 Drosophila myc regulates cellular growth during development. Cell **98:** 779-790.

JOHNSTONE, I. L., Y. SHAFI and J. D. BARRY, 1992 Molecular analysis of mutations in the Caenorhabditis elegans collagen gene dpy-7. Embo J **11:** 3857-3863.

JOHNSTONE I.L., 2000 Cuticle collagen genes expression in *Caenorhabditis elegans*. *Trends Genet.* **16:** 21–27

JONES, G. C., and G. P. RILEY, 2005 ADAMTS proteinases: a multi-domain, multi-functional family with roles in extracellular matrix turnover and arthritis. Arthritis Res Ther **7:** 160-169.

JONES, K. T., E. R. GREER, D. PEARCE and K. ASHRAFI, 2009 Rictor/TORC2 regulates caenorhabditis elegans fat storage, body size, and development through sgk-1. PLoS Biol **7:** e60.

KAMATH, R. S., M. MARTINEZ-CAMPOS, P. ZIPPERLEN, A. G. FRASER and J. AHRINGER, 2001 Effectiveness of specific RNA-mediated interference through ingested double-stranded RNA in Caenorhabditis elegans. Genome Biol **2:** RESEARCH0002.

KAUSHAL, G. P., and S. V. SHAH, 2000 The new kids on the block: ADAMTSs, potentially multifunctional metalloproteinases of the ADAM family. J Clin Invest **105:** 1335-1337.

KIMBLE J.E. and D. I., HIRSH ,1979. Post-embryonic cell lineages of the hermaphrodite and male gonads in C. elegans. Developmental Biology **70**:396-417

KIMBLE J. E. and J.G. WHITE, 1981. On the control of germ cell development in *Caenorhabditis elegans*, *Dev. Biol* **81**: 208–219

KRAMER, J. M., 1994 Structures and functions of collagens in Caenorhabditis elegans. Faseb J **8:** 329-336.

KRAMER, J. M., and J. J. JOHNSON, 1993 Analysis of mutations in the sqt-1 and rol-6 collagen genes of Caenorhabditis elegans. Genetics **135:** 1035-1045.

KRAMER, J. M., J. J. JOHNSON, R. S. EDGAR, C. BASCH and S. ROBERTS, 1988 The sqt-1 gene of C. elegans encodes a collagen critical for organismal morphogenesis. Cell **55:** 555-565.

KRISHNA, S., L. L. MADUZIA and R. W. PADGETT, 1999 Specificity of TGFbeta signaling is conferred by distinct type I receptors and their associated SMAD proteins in Caenorhabditis elegans. Development **126:** 251-260.

KUBOTA, Y., O. KIYOTAKA, T. KATSUYUKI, N. KAYO and N. KIYOJI, 2008 MIG-17/ADAMTS controls cell migration by recruiting nidogen to the basement membrane in *C. elegans* PNAS**105:** 20804–20809

KUHARA, A., H. INADA, I. KATSURA and I. MORI, 2002 Negative regulation and gain control of sensory neurons by the C. elegans calcineurin TAX-6. Neuron **33:** 751-763.

KUNO, K., C. BABA, A. ASAKA, C. MATSUSHIMA, K. MATSUSHIMA *et al.*, 2002 The Caenorhabditis elegans ADAMTS family gene adt-1 is necessary for morphogenesis of the male copulatory organs. J Biol Chem **277:** 12228-12236.

KUNO, K., and K. MATSUSHIMA, 1998 ADAMTS-1 protein anchors at the extracellular matrix through the thrombospondin type I motifs and its spacing region. J Biol Chem **273:** 13912-13917.

KUNO, K., N. KANADA, E. NAKASHIMA, F. FUJIKI, F. ICHIMURA, and K. MATSUSHIMA, 1997 Molecular cloning of a gene encoding a new type of metalloproteinase-disintegrin family protein with thrombospondin motifs as an inflammation associated gene. J. Biol. Chem. **272**: 556–562

KUNO, K., Y. OKADA, H. KAWASHIMA, H. NAKAMURA, M. MIYASAKA *et al.*, 2000 ADAMTS-1 cleaves a cartilage proteoglycan, aggrecan. FEBS Lett **478:** 241-245.

LE GOFF, C., F. MORICE-PICARD, N. DAGONEAU, L. W. WANG, C. PERROT *et al.*, 2008 ADAMTSL2 mutations in geleophysic dysplasia demonstrate a role for ADAMTS-like proteins in TGF-beta bioavailability regulation. Nat Genet. 40**:** 1119 - 1123

LEE, H. X., F. A. MENDES, P. JEAN-LOUIS and E. M. DE ROBERTIS 2009 Enzymatic regulation of pattern: BMP4 binds CUB domains of Tolloids and inhibits proteinase activity. *Genes Dev.* 2009 **23:** 2551-2562

LEEVERS, S. J., D. WEINKOVE, L. K. MACDOUGALL, E. HAFEN and M. D. WATERFIELD, 1996 The Drosophila phosphoinositide 3-kinase Dp110 promotes cell growth. Embo J **15:** 6584-6594.

LENAERS, A., M. ANSAY, B. V. NUSGENS and C. M. LAPIERE, 1971 Collagen made of extended - chains, procollagen, in genetically-defective dermatosparaxic calves. Eur J Biochem **23:** 533-543.

LETTRE, G., A. U. JACKSON, C. GIEGER, F. R. SCHUMACHER, S. I. BERNDT *et al.*, 2008 Identification of ten loci associated with height highlights new biological pathways in human growth. Nat Genet **40:** 584-591.

LEVY, A. D., J. YANG and J. M. KRAMER, 1993 Molecular and genetic analyses of the Caenorhabditis elegans dpy-2 and dpy-10 collagen genes: a variety of molecular alterations affect organismal morphology. Mol Biol Cell **4:** 803-817.

LEVY, G. G., W. C. NICHOLS, E. C. LIAN, T. FOROUD, J. N. MCCLINTICK *et al.*, 2001 Mutations in a member of the ADAMTS gene family cause thrombotic thrombocytopenic purpura. Nature **413:** 488-494.

LIANG, J., R. LINTS, M. L. FOEHR, R. TOKARZ, L. YU *et al.*, 2003 The Caenorhabditis elegans schnurri homolog sma-9 mediates stage- and cell type-specific responses to DBL-1 BMP-related signaling. Development **130:** 6453-6464.

LINTS, R., AND S. W. EMMONS, 1999 Patterning of dopaminergic neurotransmitter identity among *Caenorhabditis elegans* ray sensory neurons by a TGF b family signaling pathway and a *Hox* gene. Development, **126**, 5819-5831

LUQUE, A., D. R. CARPIZO, and M. L. IRUELA-ARISPE, 2003 ADAMTS1/METH1 inhibits endothelial cell proliferation by direct binding and sequestration of VEGF 165. J. Biol. Chem. **278**: 23656–23665

MADUZIA, L.L., A. F. ROBERTS, H. WANG, X. LIN, L. J. CHIN, C. M. ZIMMERMAN *et al.*, 2005 *C. elegans* serine-threonine kinase KIN-29 modulates TGF**β** signaling and regulates body size formation *BMC Developmental Biology* **5**:8-16

RODR´IGUEZ-MANZANEQUE, J. C., A. B. MILCHANOWSKI, E. K. DUFOUR, R. LEDUC, R. and M. L. IRUELA-ARISPE, 2000 Characterization of METH-1/ADAMTS1 processing revealstwo distinct active forms. J. Biol. Chem. **275**: 33471–33479

MAYDAN, J. S., H. M. OKADA, S. FLIBOTTE, M. L. EDGLEY and D. G. MOERMAN, 2009 De Novo Identification of Single Nucleotide Mutations in Caenorhabditis elegans Using Array Comparative Genomic Hybridization. Genetics **181:** 1673-1677.

MCKEOWN, C., V. PRAITIS and J. AUSTIN, 1998 sma-1 encodes a betaH-spectrin homolog required for Caenorhabditis elegans morphogenesis. Development **125:** 2087-2098.

MELLO, C. C., J. M. KRAMER, D. STINCHCOMB and V. AMBROS, 1991 Efficient gene transfer in C.elegans: extrachromosomal maintenance and integration of transforming sequences. Embo J **10:** 3959-3970.

MOHLER, W. A., J. S. SIMSKE, E. M. WILLIAMS-MASSON, J. D. HARDIN and J. G. WHITE, 1998 Dynamics and ultrastructure of developmental cell fusions in the Caenorhabditis elegans hypodermis. Curr Biol **8:** 1087-1090.

MONTAGNE, J., M. J. STEWART, H. STOCKER, E. HAFEN, S. C. KOZMA *et al.*, 1999 Drosophila S6 kinase: a regulator of cell size. Science **285:** 2126-2129.

MORCK, C., and M. PILON, 2006 C. elegans feeding defective mutants have shorter body lengths and increased autophagy. BMC Dev Biol **6:** 39.

MYERS, T. R., and I. GREENWALD, 2005 lin-35 Rb acts in the major hypodermis to oppose ras-mediated vulval induction in C. elegans. Dev Cell **8:** 117-123.

NAGAMATSU, Y and Y. OHSHIMA Y 2004 Mechanisms for the control of body size by a G-kinase and a downstream TGFβ signal pathway in *Caenorhabditis elegans*. *Genes Cells* **9:** 39-47

NEUFELD, T. P., and B. A. EDGAR, 1998 Connections between growth and the cell cycle. Curr Opin Cell Biol **10:** 784-790.

NEUFELD T.P., 2003. Body building: regulation of shape and size by PI3K/TOR signaling during development. Mechanisms of Development **120**: 1283-1296.

NISHIWAKI K, N. HISAMOTO and K. MATSUMOTO, 2000 A metalloprotease disintegrin that controls cell migration in Caenorhabditis elegans. Science **288:** 2205–2208

NYSTROM, J., Z. Z. SHEN, M. AILI, A. J. FLEMMING, A. LEROI *et al.*, 2002 Increased or decreased levels of Caenorhabditis elegans lon-3, a gene encoding a collagen, cause reciprocal changes in body length. Genetics **161:** 83-97.

OLDHAM, S., R. BOHNI, H. STOCKER, W. BROGIOLO and E. HAFEN, 2000 Genetic control of size in Drosophila. Philos Trans R Soc Lond B Biol Sci **355:** 945-952.

PATTERSON G.I., and R.W. PADGETT 2000 TGF ß-related pathways: roles in *Caenorhabditis elegans* development. Trends Genet **16:** 27-33

PORTER, S., I. M. CLARK, L. KEVORKIAN and D. R. EDWARDS, 2005 The ADAMTS metalloproteinases. Biochem J **386:** 15-27.

PROCKOP D. J. and K. I. KIVIRIKKO, 1995 Collagens: molecular biology, diseases, and potentials for therapy. *Annu. Rev. Biochem.* **64:**403–434

SAVAGE-DUNN C. 2001 Targets of TGFβ-related signaling in *Caenorhabditis elegans*. *Cytokine Growth Factor Rev* **12:** 305-12

SAVAGE-DUNN, C., 2005 TGF-beta signaling. WormBook**:** 1-12.

SAVAGE-DUNN, C., L. L. MADUZIA, C. M. ZIMMERMAN, A. F. ROBERTS, S. COHEN *et al.*, 2003 Genetic screen for small body size mutants in C. elegans reveals many TGFbeta pathway components. Genesis **35:** 239-247.

SAVAGE, C., P. DAS, A. L. FINELLI, S. R. TOWNSEND, C. Y. SUN *et al.*, 1996 Caenorhabditis elegans genes sma-2, sma-3, and sma-4 define a conserved family of transforming growth factor beta pathway components. Proc Natl Acad Sci U S A **93:** 790-794.

SEALS, D. F. and COURTNEIDGE, S. A. 2003The ADAMs family of metalloproteases: multidomain proteins with multiple functions. Genes Dev. **17**, 7–30

SINGARAVELU, G., H. O. SONG, Y. J. JI, C. JEE, B. J. PARK *et al.*, 2007 Calcineurin interacts with KIN-29, a Ser/Thr kinase, in Caenorhabditis elegans. Biochem Biophys Res Commun **352:** 29-35.

SOMERVILLE, R. P., J. M. LONGPRE, K. A. JUNGERS, J. M. ENGLE, M. ROSS *et al.*, 2003 Characterization of ADAMTS-9 and ADAMTS-20 as a distinct ADAMTS subfamily related to Caenorhabditis elegans GON-1. J Biol Chem **278:** 9503-9513.

SOUKAS, A. A., E. A. KANE, C. E. CARR, J. A. MELO and G. RUVKUN, 2009 Rictor/TORC2 regulates fat metabolism, feeding, growth, and life span in Caenorhabditis elegans. Genes Dev **23:** 496-511.

SULSTON J.E., E. SCHIERENBERG, J. G. WHITE, J. N. THOMSON, 1983 The embryonic cell lineage of the nematode *Caenorhabditis elegans*. *Dev Biol* **100:** 64-119

STOCKER, W., F. GRAMS, U. BAUMANN, P. REINEMER, F. X. GOMIS-RUTH *et al.*, 1995 The metzincins--topological and sequential relations between the astacins, adamalysins, serralysins, and matrixins (collagenases) define a superfamily of zinc-peptidases. Protein Sci **4:** 823-840.

SUZUKI, Y., G. A. MORRIS, M. HAN and W. B. WOOD, 2002 A cuticle collagen encoded by the lon-3 gene may be a target of TGF-beta signaling in determining Caenorhabditis elegans body shape. Genetics **162:** 1631-1639.

SUZUKI, Y., M. D. YANDELL, P. J. ROY, S. KRISHNA, C. SAVAGE-DUNN *et al.*, 1999 A BMP homolog acts as a dose-dependent regulator of body size and male tail patterning in Caenorhabditis elegans. Development **126:** 241-250.

TANG, B. L., 2001 ADAMTS: a novel family of extracellular matrix proteases. Int J Biochem Cell Biol **33:** 33-44.

THEIN, M. C., G. MCCORMACK, A. D. WINTER, I. L. JOHNSTONE, C. B. SHOEMAKER *et al.*, 2003 Caenorhabditis elegans exoskeleton collagen COL-19: an adult-specific marker for collagen modification and assembly, and the analysis of organismal morphology. Dev Dyn **226:** 523-539.

TORTORELLA, M., M. PRATTA, R. Q. LIU, I. ABBASZADE, H. ROSS *et al.*, 2000 The thrombospondin motif of aggrecanase-1 (ADAMTS-4) is critical for aggrecan substrate recognition and cleavage. J Biol Chem **275:** 25791-25797.

TORTORELLA, M. D., E. C. ARNER, R. HILLS, J. GORMLEY, K. FOK *et al.*, 2005 ADAMTS-4 (aggrecanase-1): N-terminal activation mechanisms. Arch Biochem Biophys **444:** 34-44.

TURSUN, B., L. COCHELLA, I. CARRERA, and O. HOBERT 2009 A Toolkit and Robust Pipeline for the Generation of Fosmid-Based Reporter Genes in *C. elegans.* PLoS ONE. **4:** e4625.

TYLER D.M, and N. E., BAKER, 2007 *Expanded* and *fat* regulate growth and differentiation in the *Drosophila* eye through multiple signaling pathways. Dev Biol **305:**187–201.

VAN DER KEYL, H., H. KIM, R. ESPEY, C. V. OKE and M. K. EDWARDS, 1994 Caenorhabditis elegans sqt-3 mutants have mutations in the col-1 collagen gene. Dev Dyn **201:** 86-94.

VAN DER REST M. and R. GARRONE 1991 Collagen family of proteins. *FASEB J.* **5**:2814–2823

VISSE, R. and H. NAGASE, 2003 Matrix metalloproteinases and tissue inhibitors of metalloproteinases: structure, function, and biochemistry. Circ. Res. **92**, 827–839

VON MENDE, N., D. M. BIRD, P. S. ALBERT and D. L. RIDDLE, 1988 dpy-13: a nematode collagen gene that affects body shape. Cell **55:** 567-576.

WANG X., R. E. HARRIS, L. J. BAYSTON, H. L. ASHE 2008 Type IV collagens regulate BMP signallingin Drosophila. Nature **10:**1-6.

WANG W. M., G. E. GAOXIANG, N. H., LIM, H., NAGASE, and D. S. GREENSPAN 2006 TIMP-3 inhibits the procollagen N-proteinase ADAMTS-2.The Biochemical journal **398:**515-9.

WANG, W. M., S. LEE, B. M. STEIGLITZ, I. C. SCOTT, C. C. LEBARES, M. L. ALLEN et al., 2003 Transforming growth factor-beta induces secretion of activated ADAMTS-2. A procollagen III N-proteinase.J. Biol. Chem. **278**: 19549–19557

WANG, J., R. TOKARZ and C. SAVAGE-DUNN, 2002 The expression of TGFbeta signal transducers in the hypodermis regulates body size in C. elegans. Development **129:** 4989-4998.

WANG, W. M., S. LEE, B. M. STEIGLITZ, I. C. SCOTT, C. C. LEBARES *et al.*, 2003 Transforming growth factor-beta induces secretion of activated ADAMTS-2. A procollagen III N-proteinase. J Biol Chem **278:** 19549-19557.

WATANABE, N., Y. NAGAMATSU, K. GENGYO-ANDO, S. MITANI and Y. OHSHIMA, 2005 Control of body size by SMA-5, a homolog of MAP kinase BMK1/ERK5, in C. elegans. Development **132:** 3175-3184.

WEEDON, M. N., H. LANGO, C. M. LINDGREN, C. WALLACE, D. M. EVANS *et al.*, 2008 Genome-wide association analysis identifies 20 loci that influence adult height. Nat Genet **40:** 575-583.

WILLECKE M., F. HAMARATOGLU, M., KANGO-SINGH, R., UDAN, C. L., CHEN, C., TAO, X., ZHANG and G., HALDER 2006 The Fat Cadherin acts through the Hippo tumor suppressor pathway to regulate tissue size. Current Biology 16: 2090-100.

YANG J, and J. M. KRAMER 1994. In vitro mutagenesis of Caenorhabditis elegans cuticle collagens identifies a potential subtilisin-like protease cleavage site and demonstrates that carboxyl domain disulfide. Molecular and Cellular Biology **14**: 2722-2730.

YOSHIDA S, K. MORITA, M. MOCHII and N. UENO 2001 Hypodermal expression of *Caenorhabditis elegans* TGF-β type I receptor SMA-6 is essential for the growth and maintenance of body length. *Dev Biol* **240:** 32-45